



THE PEOPLE'S DEMOCRATIC REPUBLIC OF ALGERIA  
MINISTRY OF HIGHER EDUCATION AND SCIENTIFIC  
RESEARCH



Serial N° : ...../2024

## University of Kasdi Merbah Ouargla

Faculty of Hydrocarbon, Renewable Energy, Earth and Universe Sciences

Department of Production

### Master's graduate thesis

Submitted by:

**LAHCENE Saidi, YOUCEF Djouber, YOUNES Bounoua**

To obtain the master's degree

Specialty: Hydrocarbons

Option: Professional Production

-THEME-

**Performance study: water coning in Amassak  
field - Ain Aminas.**

Defended on: 10 /06 / 2024

**Jury members:**

HALIMA Baziou	MAB	UKMO	President
AMMAR Mahsouel	MCA	UKMO	Examiner
DJAMILA Boufades	MCA	UKMO	Supervisor
ZAKARIA Adjou	Ph. D	UKMO	Co-Supervisor

Academic year: 2023/2024

# *Acknowledgments*

We would thank Allah for the strength, patience, and motivation he provides us to accomplish this work, thanks to you God for everything you gave, give, and will give to us, and for everything you took, take, and will take from us.

We want to extend our heartfelt appreciation to our supervisor Miss Djamila Boufades and our co-supervisor Mr. Zakaria Adjou who were always by our side during the journey.

A special thanks to the jury members Miss HALIMA Baziou and Mr AMMAR Mahsouel for their time and invaluable contribution to the process.

We want to express our sincere gratitude for our teachers, professors, and all the members of the production department of the University of Kasdi Merbah Ouargla for their steadfast companionship during these years.

To Mr. Mehdi Al Aoufi, Mr. Smail Tayeb, Mr. Mahmoud, Mr. Abd Elkrim, Mr. Yacine Dahmani, Mr. Mouiz and their colleagues in Sonatrach DP TFT who provided us with the main resources so we could accomplish this work.

Our thanks and respect for our colleagues in the university and for all the people who have willingly helped us out with their abilities.

# *Dedication*

Alhamdulillah, all praises to Allah for the strengths and His blessing in completing this thesis.

This work is dedicated to my great parents, who never stop giving of themselves in countless ways, my beloved brother and sisters, for the endless encouragement, my sweet angels: Malek, Imran, and Oussaid. I am forever grateful for your presence in my life.

To my friends, it has been an honor and a privilege to meet you and share these past five years together. Your friendship, support, and laughter have made this journey truly memorable. Thank you for always being there, through both the highs and the lows.

To my thesis partners, Youcef and Younes. I am immensely proud to have been a part of this team, your hard work and collaboration have been essential to the completion of this thesis. Working together with you has been an inspiring and rewarding experience. Thank you for your commitment and teamwork.

To all those who have touched my life in profound ways, your presence, whether big or small, has left an indelible mark on my heart. Your belief in me has given me the strength to persevere. Thank you for being a part of my story and for inspiring me to reach new heights.

**Lahcene Saidi**

## *Dedication*

This work is dedicated to my beloved parents, who are my source of motivation and strength every second I think of giving up.

To my brother Khaled and my two little sisters Meriem and Alia with all love, to my family who shared their words of advice and encouragement so I can accomplish this work.

To Petroleum Club Ouargla, and to the incredible people I met in, to Chahla, Nouha, Hanine, Narimane, Amine, Anis, Zaki, Imade, and Smail, for the unforgettable memories we made, with all hope things have not come yet to an end.

To my friends along the journey, Younes, Lahcene, Akram, Walid, Abd El Badie, Abd Assamad, Kader, Oussama, Rida, Issam, Fethi, and Mokhtar.

To the special people, to Hichem, Omar, Adel, Bachir, Mostapha, Farouk, Mohammed, Ouassma, and Narimane Abla for making my life every day better and better.

**Youcef Djouber**

# *Dedication*

Firstly, I thank God for his blessings.

I would like to express my deepest gratitude and dedicate this thesis to my loving family, who have been my pillars of strength throughout this journey.

I dedicate this thesis to my mother and father, whose prayer, support and guidance have been essential in my success.

I also extend my gratitude to my brothers, Khaled, Youcef, and Yacine, for their motivation and inspiration.

Additionally, I would like to acknowledge my sisters, who have been a source of love and care.

Furthermore, I would like to thank my teammates, Lahcene and Youcef, for their commitment and hard work make this journey easier.

Lastly, I would like to extend my heartfelt gratitude to my dear friends from the university residence, including Abdessamed, Abdelbadie, Abdelkader, Abdelraouf, Akram, Idriss, Rida, Sifeddine, Oussama, and Walid, for the unforgettable memories and cherished moments we shared during our time at the residence.

**Younes Bounoua**

## ملخص

تعتبر مشكلة مخروط المياه من أهم التحديات أثناء إنتاج النفط، حيث يحدث تحرك منطقة التلامس بين النفط والماء نحو ثقب البئر لتشكل مخروط. من خلال اختيار خمسة آبار منتجة، AMA73، AMA75، AMA69، HBDA1 و HBDA6. يقوم هذا البحث بتحليل أداء حقل أماساك لفهم ومعالجة تأثير هذه الظاهرة. يهدف هذا البحث إلى عرض تأثير نسبة المياه المنتجة على معدلات إنتاج الزيت باستعمال برنامج بروسبر، وتشخيص ظاهرة مخروط المياه باستخدام منحني تشان، وتقييم تقنيات الإنتاج التدخل. تشير النتائج إلى أن تنفيذ آبار ذات نصف قطر قصير (HBDA6) قلت نسبة المياه المنتجة فيه من 60.98% إلى 0% والحفاظ على معدلات إنتاج النفط قريبة من تدفقات إنتاج الزيت الحرجة يمكن أن يؤخر وقت اختراق المياه ويقلل من التأثير الاقتصادي.

**كلمات مفتاحية:** أداء، مخروط المياه، نسبة المياه المنتجة، تدفقات الحرجة، وقت اختراق المياه.

## Résumé

Le coning d'eau est l'un des principaux problèmes lors de la production du pétrole, qui correspond au déplacement de l'interface eau-huile vers les abords du puits, formant un cône. En choisissant cinq puits producteurs AMA73, AMA75, AMA69, HBDA1 et HBDA6, cette étude analyse la performance du gisement d'Amassak pour comprendre et atténuer les effets de ce phénomène, elle est aussi à mettre en évidence les impacts du pourcentage d'eau produite sur les taux de production d'huile en utilisant le logiciel Prosper, diagnostiquer ce phénomène, avec le tracé de Chan, et évaluer les techniques de production et d'intervention. Les résultats indiquent que la mise en place des puits short radius (HBDA6, le pourcentage d'eau produite a été réduite de 60,98% à 0%) et le maintien des taux de production d'huile près des débits critiques peuvent retarder le temps de percée et minimiser l'impact économique.

**Mot clés :** Performance, coning d'eau, pourcentage d'eau produite, débit critique, temps de percée.

## Abstract

Water coning is one of the major problems during oil production, which is the movement of the oil-water interface towards the well boundaries forming a cone. By choosing five producing wells AMA73, AMA75, AMA69, HBDA1 and HBDA6, this study analyses the performance of the Amassak field to understand and mitigate the effects of this phenomenon. This research aims to display the impacts of water cut on the oil production rates using Prosper software, diagnose the water coning with Chan plot, and evaluate production and mitigation techniques. The results indicate that implementing short-radius wells (HBDA6 water cut reduced from 60.98% to 0%) and maintaining oil production rates near critical thresholds can delay water breakthrough time and minimize the economic impact.

**Keywords:** Performance, water coning, water cut, critical threshold, water breakthrough time.

## Table of contents

Acknowledgments .....	I
Dedication .....	II
Abstract .....	V
Table of contents .....	VI
List of figures .....	IX
List of tables .....	XI
List of abbreviation .....	XII
General introduction.....	1

### Chapter I: fundamentals of porous medium properties.

I.1 Reservoir petrophysical properties .....	3
I.1.1 Porosity.....	3
I.1.2 Permeability.....	4
I.1.3 Saturation.....	4
I.1.4 Wettability .....	5
I.1.5 Rock compressibility .....	6
I.1.6 Capillary pressure .....	6
I.1.7 Relative permeability.....	7
I.1.8 Mobility ratio.....	8
I.2 Fundamentals of reservoir fluid flow.....	8
I.2.1 Reservoir fluids .....	8
I.2.2 Flow regimes .....	9
I.2.3 Flow geometries .....	10
I.2.4 Basic PVT parameters .....	11
I.2.5 Well Testing .....	12

### Chapter II: drive mechanisme and well performance.

II.1 Drive mechanisms .....	14
-----------------------------	----

II.1.1	Natural water drive .....	14
II.1.2	Solution gas drive .....	14
II.1.3	Gas-cap drive .....	14
II.1.4	Compaction drive .....	14
II.2	Well performance .....	14
II.2.1	Inflow performance relationship .....	14
II.2.2	Outflow performance .....	16
II.2.3	Operating point .....	18
II.3	Artificial lift .....	19
II.3.1	Electrical Submersible Pumps .....	21
II.3.2	Gas lift .....	23

**Chapter III: water coning and its remedial techniques.**

III.1	Water coning .....	26
III.2	The physics of water coning .....	26
III.3	Water control diagnostics plots .....	27
III.4	Prediction of water coning .....	29
III.4.1	Calculation of critical oil rate .....	29
III.4.2	Calculation of the breakthrough time .....	33
III.5	Water coning control methods .....	34
III.5.1	Mechanical and completion methods .....	35
III.5.2	Chemical methods .....	41

**Chapter IV: optimizing oil production in the Amassak field: diagnosing and mitigating water coning.**

IV.1	Presentation of the TFT region .....	42
IV.1.1	Amassak field background .....	43
IV.1.2	HBDA field background .....	44
IV.1.3	DATA collection .....	46



IV.2	The impact of water cut on the oil production rate .....	47
IV.2.1	History analysis of water cut and oil production rate .....	47
IV.2.2	Simulation Analysis using PROSPER .....	49
IV.3	Case study 1: Problem diagnosis.....	51
IV.3.1	Chan plot .....	51
IV.3.2	Determination of critical production rate.....	52
IV.3.3	Water Breakthrough Time.....	52
IV.3.4	Discussion of results .....	54
IV.4	Case study 02: Water coning risks in artificial lift operations .....	55
IV.4.1	Discussion of results .....	56
IV.5	Case study 3: Short radius as a mitigation technique.....	56
IV.5.1	Discussions of results.....	58
	Conclusion and Recommendations .....	50
	References .....	62
	Appendices	

## List of figures

Figure I-1: Diagram display primary porosity at different particle sizes. ....	3
Figure I-2: Diagram shows type of secondary porosity existing in reservoir rock.....	4
Figure I-3: Illustration of wettability. ....	5
Figure I-4: The compaction effects before and after development.....	6
Figure I-5: Capillary pressure in oil-water system . ....	7
Figure I-6: Flow regimes types .....	10
Figure I-7: flow geometries types .....	10
Figure II-1: IPR typical curve .....	16
Figure II-2: VLP typical curve .....	18
Figure II-3: Operating point (intersection between IPR and VLP curves).....	19
Figure II-4: Schematic Pressure Profile for Production System (natural flow) .....	20
Figure II-5: Schematic Pressure Profile for Production System (artificial lift).....	20
Figure II-6: Artificial lift method .....	21
Figure II-7: Schematic view of ESP. ....	22
Figure II-8: Schematic view of GL method .....	23
Figure III-1: water coning in vertical wells .....	27
Figure III-2: Multi-layer channelling WOR and WOR derivatives.....	28
Figure III-3: Bottom-water coning WOR and WOR derivatives .....	28
Figure III-4: Bottom water coning with late time channelling. ....	29
Figure III-5: Critical rate correlation .....	32
Figure III-6: Using plug to shut off the production of water from the bottom. ....	35
Figure III-7: Two packers above and below a blank pipe to shut-off water production from middle and upper part. ....	36
Figure III-8: intelligent well completion .....	37
Figure III-9: DOWS with hydro cyclone separator. ....	38
Figure III-10: DOWS with gravity separator.....	38
Figure III-11: Schematic of Typical DWS Completion.....	39
Figure III-12: Schematic of Typical DWL Completion. ....	40
Figure IV-1: Geographical Location of the Tin Fouyé Tabenkourt zone.....	42
Figure IV-2: Distribution of oil fields in the Illizi Basin .....	42
Figure IV-3: Geological location of the 18 perimeters in the TFT area. ....	43
Figure IV-4: Well locations in HBDA field . ....	45

Figure IV-5: Impact of water cut on production flow rate in AMA 73.....	48
Figure IV-6: Impact of water cut on production flow rate in AMA 75.....	48
Figure IV-7: PROSPER software interface and utilizations .....	49
Figure IV-8: Water cut sensitivity analyses.....	50
Figure IV-9: Well AMA 73 Chan plot.....	51
Figure IV-10: Well AMA 75 Chan plot.....	51
Figure IV-11: predicting water breakthrough time with difference flow rates for AMA 73....	53
Figure IV-12: predicting water breakthrough time with difference flow rates for AMA 75....	54
Figure IV-13: Oil production rate and water cut performance before and after ESP installation in the well HBDA1. ....	55
Figure IV-14: Impact of GL on the performance of oil production rate and water cut in the well AMA69. ....	55
Figure IV-15: Well HBDA6 technical sheet.....	57
Figure IV-16: Oil rate and water cut performance in HBDA6. ....	58

## **List of tables**

Table II-1: Advantages and disadvantages of the ESP are as follows .....	22
Table II-2: Advantages and disadvantages of the gas lift method are as follows: .....	24
Table IV-1: Reservoir fluid properties .....	56
Table IV-2: Reservoir rock properties.....	56
Table IV-3: Critical Oil Rate Correlation Results, Well AMA 73.....	52
Table IV-4: Critical Oil Rate Correlation Results, Well AMA 75.....	52
Table IV-5: TIME BREAKTHROUGH .....	53

### *List of abbreviation*

<b>A</b>	Cross-sectional area across which flow occurs, cm <sup>2</sup> .
<b>A</b>	Cross-sectional area, ft <sup>2</sup> .
<b>Bo</b>	Oil formation volume factor, res. bbl/STB.
<b>BHP</b>	Bottomhole pressure.
<b>Bg</b>	Gas formation volume factor, ft <sup>3</sup> /scf.
<b>C</b>	compressibility, Pa <sup>-1</sup> .
<b>d</b>	Pipe inside diameter, ft.
<b>dp/dL</b>	Pressure drop per unit length, atm/cm.
<b>DWS</b>	Downhole water sink.
<b>DWL</b>	Downhole water loop.
<b>DOWS</b>	Downhole oil-water separation.
<b>ESP</b>	Electric Submersible Pumps.
<b>FBHP</b>	Flowing bottom hole pressure.
<b>F</b>	Friction factor.
<b>GLR</b>	Gas-to-liquid ratio, ft <sup>3</sup> /bbl.
<b>GL</b>	Gaz Lift.
<b>GLVs</b>	Gas Lift Valves.
<b>GOR</b>	Gas-to-oil ratio, scf/bbl.
<b>g</b>	Gravity constant, N·m <sup>2</sup> /kg <sup>2</sup> .
<b>HBDA</b>	Hassi Belhouda.
<b>h</b>	Oil column thickness, ft.
<b>h<sub>p</sub></b>	Perforated interval, ft.
<b>h</b>	Thickness, ft.
<b>h</b>	Pay thickness, ft.
<b>h<sub>p</sub></b>	Penetration interval, ft.
<b>IPR</b>	Inflow Performance Relationship.
<b>ICV</b>	Inflow Control Valves.
<b>IPM</b>	Integrated Production Modelling.
<b>K</b>	Permeability, m <sup>2</sup> or mD.
<b>(k<sub>h</sub>)</b>	Horizontal permeabilities, mD.
<b>(k<sub>v</sub>)</b>	Vertical permeability, mD.
<b>(k<sub>ro</sub>)</b>	Relative oil permeability.
<b>(k<sub>rw</sub>)</b>	Relative water permeability.

<b>k</b>	Effective permeability, mD.
<b>k<sub>o</sub></b>	Effective oil permeability, mD.
<b>K<sub>w</sub></b>	Effective water permeability, mD.
<b>K<sub>g</sub></b>	Effective gas permeability, mD.
<b>K<sub>r</sub></b>	Relative permeability.
<b>k<sub>a</sub></b>	Absolute permeability, mD.
<b>(k<sub>ro</sub>)<sub>swc</sub></b>	Oil relative permeability at connate water saturation.
<b>(k<sub>rw</sub>)<sub>sor</sub></b>	Water relative permeability at residual oil saturation.
<b>L</b>	distance, ft.
<b>M</b>	Mobility.
<b>PVT</b>	Pressure, Volume, Temperature.
<b>P<sub>c</sub></b>	Capillary pressure.
<b>P<sub>nwt</sub></b>	Pressure of the nonwetting phase.
<b>P<sub>wt</sub></b>	Pressure of the wetting phase.
<b>p</b>	Pressure, psia.
<b>p<sub>2</sub></b>	External pressure, psia.
<b>p<sub>1</sub></b>	Bottom-hole flowing pressure, psia.
<b>PI</b>	Productivity index.
<b>p<sub>R</sub></b>	Average reservoir pressure, psi
<b>p<sub>wf</sub></b>	Flowing bottomhole pressure, psi
<b>q</b>	Flow rate through the porous medium, cm <sup>3</sup> /sec.
<b>Q</b>	Flow rate, bbl/day.
<b>(Q<sub>g</sub>)<sub>p,T</sub></b>	The gas production rate, scf/day or m <sup>3</sup> /day.
<b>(Q<sub>o</sub>)<sub>p,T</sub></b>	The oil production rate, bbl/day or m <sup>3</sup> /day.
<b>Q<sub>oc</sub></b>	Critical oil rate, STB/day.
<b>q<sub>curve</sub></b>	Critical production rate from Chaney's curves, RB/D.
<b>Q<sub>cd</sub></b>	Dimensionless critical flow rate (it is correlated with the dimensionless radius $r_D$ , and fractional well penetration ratio ( $h_p / h$ )).
<b>r</b>	Capillary radius, ft.
<b>r<sub>2</sub></b>	External or drainage radius, ft.
<b>r<sub>1</sub></b>	Wellbore radius, ft.
<b>Rs</b>	The solution gas-oil ratio, scf/STB.
<b>r<sub>e</sub></b>	Drainage radius of well, ft.
<b>r<sub>w</sub></b>	Radius of wellbore, ft.

<b><math>r_D</math></b>	Dimensionless radius.
<b>Re</b>	Reynolds number.
<b>Rpm</b>	Rotation Par Minute.
<b>So</b>	Oil saturation, percent.
<b>Sw</b>	Water saturation, percent.
<b>SG</b>	Gas saturation, percent.
<b>T</b>	Temperature, °C.
<b>TFT</b>	Tin foyé tabenkourt.
<b>TFT</b>	Tin foyé tabenkourt.
<b>(<math>t_D</math>)<sub>BT</sub></b>	Dimensionless breakthrough time.
<b>(<math>t_D</math>)<sub>BT</sub></b>	Dimensionless breakthrough time.
<b><math>t_{BT}</math></b>	Time to breakthrough, days.
<b>V</b>	Volume, bbl.
<b>(<math>V_o</math>)<sub>P,T</sub></b>	The volume of oil at reservoir pressure and temperature (also includes gas in solution), bbl.
<b>(<math>V_o</math>)<sub>sc</sub></b>	The volume of oil at standard conditions, stock tank barrel (STB, always reported at standard conditions).
<b>(<math>V</math>)<sub>P,T</sub></b>	The volume of gas at reservoir pressure and temperature, ft <sup>3</sup> .
<b>(<math>V</math>)<sub>sc</sub></b>	The volume of gas at standard conditions, scf.
<b>VLP</b>	Vertical Lift Performance.
<b>V</b>	Fluid velocity, m/s.
<b>WOR</b>	Water-Oil Ratio.
<b>WOR'</b>	Derivative of water-Oil Ratio.
<b>WDI</b>	Water drainage interval.
<b>WRI</b>	Water re-injection interval.
<b>Z</b>	The dimensionless cone height.
<b><math>\phi</math></b>	Porosity, percent.
<b><math>\sigma</math></b>	Gas-water surface tension, dynes/cm.
<b><math>\theta</math></b>	Contact angle.
<b><math>\mu</math></b>	Viscosity, cp.
<b><math>\mu_o</math></b>	Oil viscosity, cp.
<b><math>\rho</math></b>	Density of fluid, kg/m <sup>3</sup> or lb/ft <sup>3</sup> .
<b><math>\beta</math></b>	Pipe inclination angle, measured from horizontal.
<b><math>\rho_w</math></b>	Water density, lb/ft <sup>3</sup> .

$\rho_g$  Gas density, lb/ft<sup>3</sup>.  
 $\rho_o$  Oil density, lb/ft<sup>3</sup>.



# *GENERAL INTRODUCTION*

## General introduction

The global energy economy heavily relies on oil production, which fuels industrial growth and provides essential resources for transportation, heating, and electricity generation. However, the efficiency of oil extraction is often challenged by technical issues and associated costs. If this oil production challenge is not mitigated, it can lead to less oil recovery and ultimately result in early abandonment of the hydrocarbon field(s) and/or well(s). A major problem in oil production is the accompanying water production. Water production may come in the form of a tongue, cone, cusp or a combination of all. Which can result from natural reservoir characteristics or production-induced changes [1] [2].

Among the causes of high-water production rates is water coning, a phenomenon where water from an underlying aquifer intrudes into the oil production well, leading to a substantial increase in water production and a corresponding decline in oil output. This phenomenon not only poses technical challenges by complicating well management and reducing oil recovery efficiency, but also escalates economic issues by raising operational costs and affecting the overall profitability of the oil field [3].

The Amassak oil field which located in the Tin Fouyé Tabankort region of the Algerian Sahara, in the Illizi province, has not been spared the challenge of water coning. This phenomenon poses a real threat to the Amassak oil field's performance on multiple fronts. The consequences of water coning extend far beyond technical complexities. Managing wells with water breakthrough becomes significantly more challenging, and the overall oil recovery efficiency drops.

### **Problem statement**

The motivation behind this research stems from the significant impact of water coning on oil production. Specifically, the closure of 25 wells in the Amassak field and 2 wells in the HBDA field due to high water cut issues has affected the annual production objectives.

This thesis addresses several questions regarding the problem of water coning in the Amassak oil field:

- What is the impact of water cut on oil production rates in the Amassak oil field?
- What diagnostic methods can be used to identify water coning phenomenon?
- How do different production methods influence the severity of water coning?
- Which strategies are most effective in delaying the onset of water breakthrough?

Answering these questions allows us to develop strategies to optimize field performance, and ensure long-term production efficiency.

### Main objectives of the thesis

- Provide clarity on the relationship between production decrease and water coning.
- Investigate the relationship between oil production rates and the critical rate, the maximum rate at which oil can be extracted before water breakthrough becomes a significant issue.
- Analyze how different artificial lift methods, such as gas lift or electric submersible pumps, impact the behaviour of water coning. Understanding this effect would help optimizing production strategies.
- Understand the effectiveness of well intervention techniques in mitigating water coning, such as short-radius, for future well management decisions.

### Structure of the thesis

The thesis began by highlighting the primary challenge encountered in the Amassak field, which revolves around water production, its sources, and implications, and subsequently delved into outlining the objectives of this study.

This work is organized into four chapters which are:

**Chapter I:** Fundamentals of porous medium properties – Explores the essential properties of the reservoir that influence water coning, including rock properties and fluid properties.

**Chapter II:** Drive mechanisms and well performance – Discusses the different drive mechanisms, and essential aspects of well performance, including artificial lift methods.

**Chapter III:** Water coning and its remedial techniques - Reviews existing research on water coning, including its causes, impacts, and strategies for management.

**Chapter IV:** Optimizing oil production in the Amassak field: diagnosing and mitigating water coning - Presents detailed case studies of the Amassak oil field under investigation, including diagnosis of water coning phenomenon, evaluation of production methods, and results from mitigation strategies.

The thesis concluded by highlighting the negative impacts of water coning on the performance of the Amassak oil field, presenting key results, and providing detailed recommendations for mitigating water coning and optimizing oil production in the field.

*Chapter I*  
*Fundamentals of porous*  
*medium properties*

## I.1 Reservoir petrophysical properties

### I.1.1 Porosity

The porosity of a rock is a measure of the storage capacity (pore volume) that is capable of holding fluids. Quantitatively, the porosity is the ratio of the pore volume to the total volume (bulk volume). This important rock property is determined mathematically by the following generalized relationship (Eq I-1) [4].

$$\phi = \frac{\text{pore volume}}{\text{bulk volume}} \quad \text{I-1}$$

Where

$\phi$ : porosity.

#### I.1.1.1 Classification of porosity:

There are two main types of porosity:

- **Absolute porosity:** The ratio of total pore space to bulk volume, including isolated pores.
- **Effective porosity:** The interconnected pore space that can transmit fluids, excluding isolated pores. This is the porosity used in reservoir engineering calculations [4].

Porosity can also be classified geologically:

- **Primary porosity:** The original porosity from deposition, including intergranular (between grains) and intragranular (within grains) porosity.
- **Secondary porosity:** Porosity that develops later, often enhancing the rock's porosity. It can result from dissolution, fracturing, or other diagenetic processes [5].

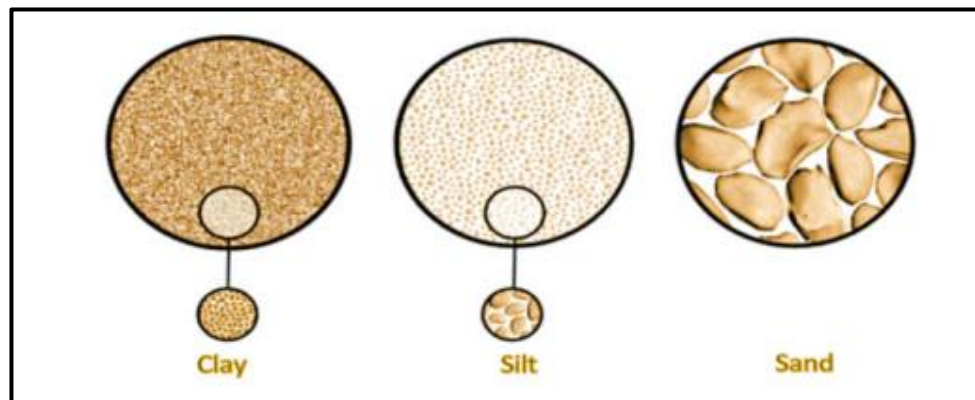


**Figure I-1:** Diagram displays primary porosity at different particle sizes [5].

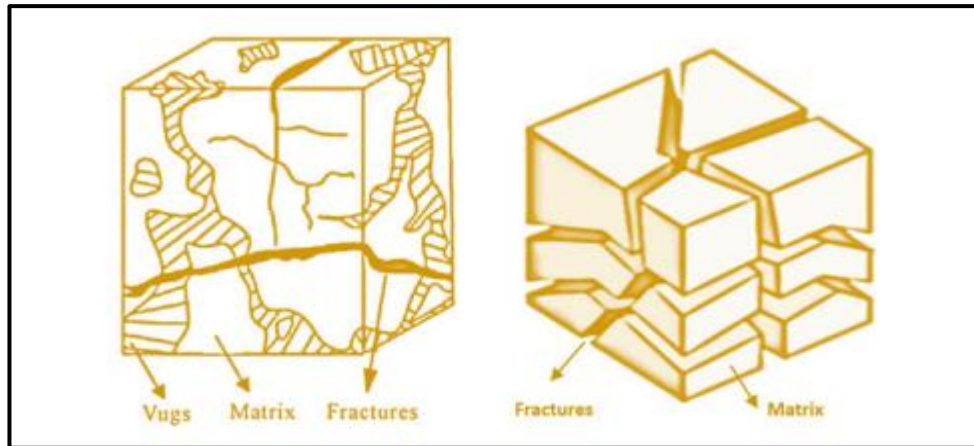


**Figure I-2:** Diagram shows types of secondary porosity existing in reservoir rock [5].

### I.1.2 Permeability

Permeability is a measure of a rock's ability to transmit fluids, and is a critical property for evaluating hydrocarbon reservoirs. It is defined by Darcy's law (Eq I-2), which relates flow rate, pressure drop, fluid viscosity, and rock properties:

$$q = -\frac{kA}{\mu} \frac{dp}{dL} \quad \text{I-2}$$

Where

**q:** flow rate through the porous medium, cm<sup>3</sup>/s.

**A:** cross-sectional area across which flow occurs, cm<sup>2</sup>.

**k:** permeability, Darcy.

**μ:** viscosity of the flowing fluid, cp.

**dp/dL:** pressure drop per unit length, atm/cm (All units are in practical system).

Permeability depends on factors like pore size, connectivity, and rock type. Typical values range from less than 1 md (very low) to over 500 md (excellent).

Routine core analysis is generally concerned with plug samples drilled parallel to bedding planes and, hence, parallel to direction of flow in the reservoir. These yield horizontal permeabilities ( $k_h$ ).

The measured permeability on plugs that are drilled perpendicular to bedding planes are referred to as vertical permeability ( $k_v$ ).

This measured permeability at 100% saturation of a single phase is called the absolute permeability of the rock [4].

### I.1.3 Saturation

Saturation is defined as that fraction, or percent, of the pore volume occupied by a particular fluid (oil, gas, or water). This property is expressed mathematically by the following relationship (Eq I-3) [4].

$$\text{Fluid Saturation} = \frac{\text{Total volume of the fluid}}{\text{Pore volume}} \quad \text{I-3}$$

The oil, water and gas saturation are:

$$S_w = \frac{V_w}{V_p} \quad \text{I-4}$$

$$S_o = \frac{V_o}{V_p} \quad \text{I-5}$$

$$S_G = \frac{V_G}{V_p} \quad \text{I-6}$$

Expressed in percent, with

$$S_w + S_o + S_G = 100\% \quad \text{I-7}$$

Knowing the volumes of oil and gas in place in a reservoir requires knowing the saturations at every point, or at least a satisfactory approximation.

### I.1.4 Wettability

Wettability is defined as the tendency of one fluid to spread on or adhere to a solid surface in the presence of other immiscible fluids [4].

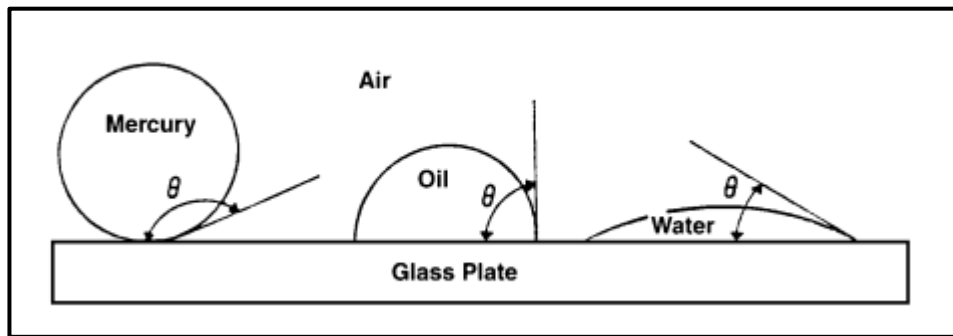


Figure I-3: Illustration of wettability [4].

#### I.1.4.1 Types of wettability:

Wettability can be classified into several types, including:

- **Water-wet:** Water occupies the small pores and contacts the majority of the rock surface.
- **Oil-wet:** Oil occupies the small pores and contacts the majority of the rock surface.
- **Intermediate wettability:** The rock has no overall preference for either oil or water.
- **Mixed wettability:** Areas of the interconnected pore space are water-wet, while the remaining surfaces are oil-wet.

#### I.1.4.2 Factors affecting wettability:

The wettability of a reservoir depends on several factors, including:

- Oil composition.
- Rock mineralogy.
- The pH of the formation brine.

- Pressure and temperature.
- Thickness of the connate water layer.

### I.1.5 Rock compressibility

Compressibility is a physical fact, which has a major function in the petroleum production system. The main compressibility effective on reservoir rock is due to two factors, known as, expansion of the rock grains, because the in-situ fluid pressure drops, and the extra formation compaction brought about [5].

Rock compressibility is expressed by the following relationship (Eq I-8):

$$C = \frac{1}{v} \left( \frac{dv}{dP} \right) T \quad \text{I-8}$$

#### I.1.5.1 Effect of rock compressibility on field development

Rock compressibility acts as an important drive mechanism in the production system, as pressure drops cause rock grains to move closer together. However, this compaction can also have negative impacts:

- Reduced porosity and permeability, limiting hydrocarbon flow.
- Potential for sand production and equipment damage.

This effect is shown in Figure I-4 [5].

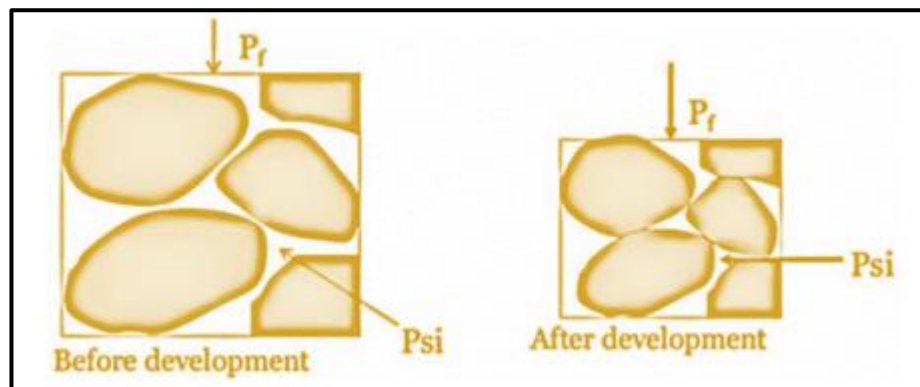


**Figure I-4:** The compaction effects before and after development [5].

### I.1.6 Capillary pressure

Capillary pressure is the pressure difference across the interface between two immiscible fluids in a porous medium. It arises due to the tendency of a liquid to rise or fall in a capillary tube, known as capillarity, which is a function of adhesion tension [6].



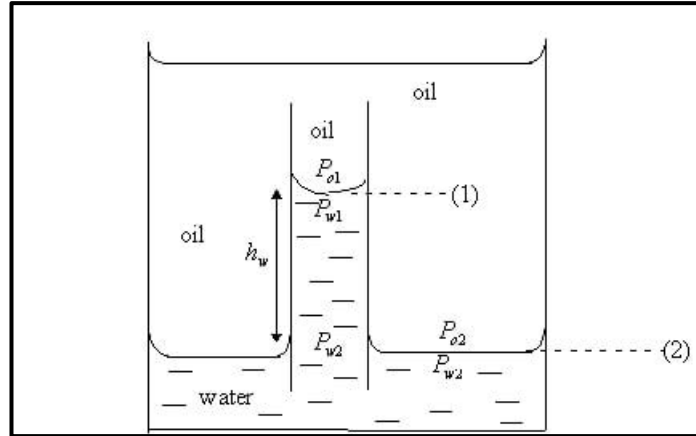


**Figure I-5:** Capillary pressure in oil-water system [7].

The capillary pressure can be expressed as (Eq I-9):

$$P_c = p_{nwt} - p_w \quad \text{I-9}$$

or in terms of the surface and interfacial tension (Eq I-10):

$$P_c = \frac{2\sigma \cos \theta}{r} \quad \text{I-10}$$

Where

$P_{nwt}$ : pressure of the nonwetting phase.

$P_w$ : pressure of the wetting phase.

$\sigma$ : gas-water surface tension, dynes/cm.

$r$ : capillary radius, cm.

$\theta$ : contact angle.

$P_c$ : capillary pressure.

### I.1.7 Relative permeability

When dealing with more than one fluid in a porous medium, the concept of single-phase permeability is no longer valid to characterize the flow in that system and thus an extension of Darcy's law is required. Relative permeability ( $k_r$ ) is a fundamental concept in reservoir engineering that quantifies the ease of one fluid to flow in the presence of another immiscible fluid within a porous medium. When discussing relative permeability, two parameters need to be discussed:

- **Absolute permeability ( $k$ )**, which is a measure of the ease of one fluid to flow in a porous medium.
- **Effective permeability**, which is the capacity of a porous medium to conduct specific fluids when multiple fluids are present ( $k_w$  for water,  $k_o$  for oil,  $k_g$  for gas) [6].

In terms of equations: The relative permeability of water ( $k_{rw}$ ) is defined as (Eq I-11):

$$k_{rw} = \frac{k_w}{k} \quad \text{I-11}$$

Similarly, the relative permeability of oil ( $k_{ro}$ ) is defined as:

$$k_{ro} = \frac{k_o}{k} \quad \text{I-12}$$

### I.1.8 Mobility ratio

The mobility is defined by the movement of one fluid displacing another fluid. This parameter,  $M$ , during aqueous displacement is given by the equation (Eq I-13):

$$M = \frac{\frac{k_{rw}}{\mu_w}}{\frac{k_{ro}}{\mu_o}} \quad \text{I-13}$$

Where

$M$ : the mobility.

$k_{rw}$ : the relative permeability of water.

$\mu_w$ : the viscosity of water, cp.

$k_{ro}$ : the relative permeability of oil.

$\mu_o$ : the viscosity of oil, cp.

Sweep efficiency improves as this value decreases, and having  $M$  less than 1 is desirable when light oils are displaced by brine. Furthermore, if the  $M$  factor is greater than 1, instability can occur, leading to viscous fingering [8].

## I.2 Fundamentals of reservoir fluid flow

Fluid flow in the porous medium is affected by various forces, and its essence is to consume energy and produce fluid through the wellbore. The relationship between energy and flow rate becomes the most important problem in flow mechanics through porous media. The mathematical forms of these relationships will vary depending on the characteristics of the reservoir. The primary reservoir characteristics that must be considered include:

- Types of fluids in the reservoir.
- Flow regimes.
- Reservoir geometry.
- Number of flowing fluids in the reservoir [4].

### I.2.1 Reservoir fluids

Petroleum reservoir fluids from a very generic standpoint broadly refer to the hydrocarbon phase and the water phase that exist under a variety of temperature and pressure conditions in subsurface formations or petroleum reservoirs. Although petroleum reservoir fluids are conventionally classified into the following types:

- Black oils.

- Volatile oils.
- Gas condensates or retrograde gases.
- Wet gases.
- Dry gases.

There are two factors that determine the behaviour of a reservoir containing any of these types of fluid as pressure and temperature change.

- Fractional split into gas and oil phases, and composition of these phases.
- Volume dependence on pressure and temperature of the two phases [9].

### I.2.2 Flow regimes

There are three types of flow regimes that must be recognized in order to describe the fluid flow behavior and reservoir pressure distribution as a function of time (Figure I-6).

#### I.2.2.1 Steady-state flow

The flow regime is identified as a steady-state flow if the pressure at every location in the reservoir remains constant, i.e., does not change with time. Mathematically, this condition is expressed as (Eq I-14):

$$\left(\frac{\delta p}{\delta t}\right) = 0 \quad \text{I-14}$$

#### I.2.2.2 Unsteady-state flow

It is defined as the fluid flowing condition at which the rate of change of pressure to time at any position in the reservoir is not zero or constant. This definition suggests that the pressure derivative to time is essentially a function of both position  $i$  and time  $t$ , thus (Eq I-15):

$$\left(\frac{\delta p}{\delta t}\right) = f(i, t) \quad \text{I-15}$$

#### I.2.2.3 Pseudo steady-state flow

It is when the pressure at different locations in the reservoir is declining linearly as a function of time, i.e., at a constant declining rate. Mathematically, this definition states that the rate of change of pressure to time at every position is constant (Eq I-16) [4].

$$\left(\frac{\delta p}{\delta t}\right) = cst \quad \text{I-16}$$

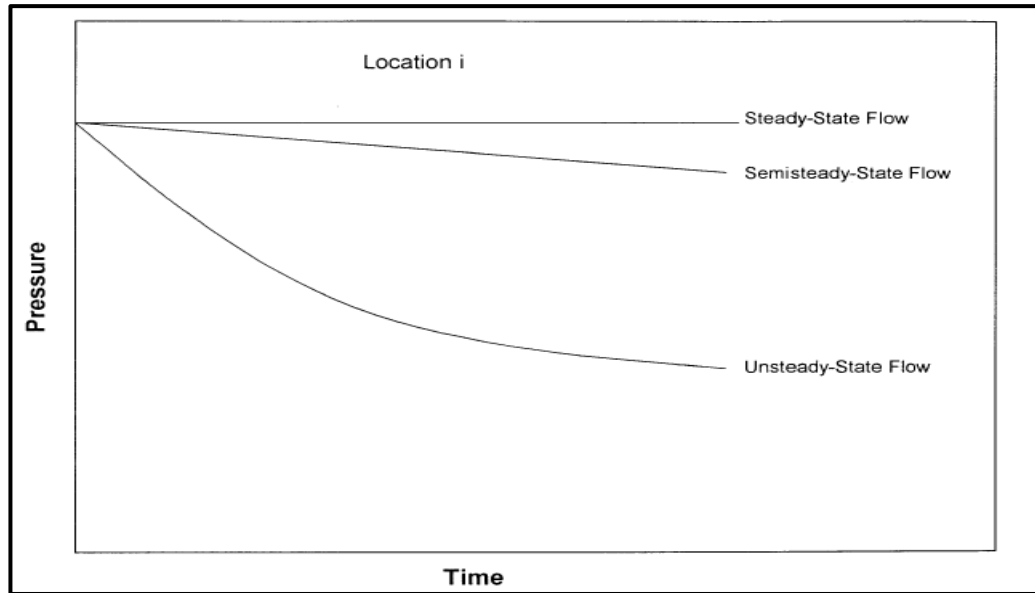


Figure I-6: Flow regimes types [4].

### I.2.3 Flow geometries

Reservoir geometries are essential in several aspects of petroleum engineering and reservoir management (Figure I-7). These geometries dictate how fluids flow within the reservoir, influencing factors such as recovery efficiency, well placement, and production strategies. There are three common types of flow geometries:

- Linear flow.
- Radial flow.
- Spherical flow.

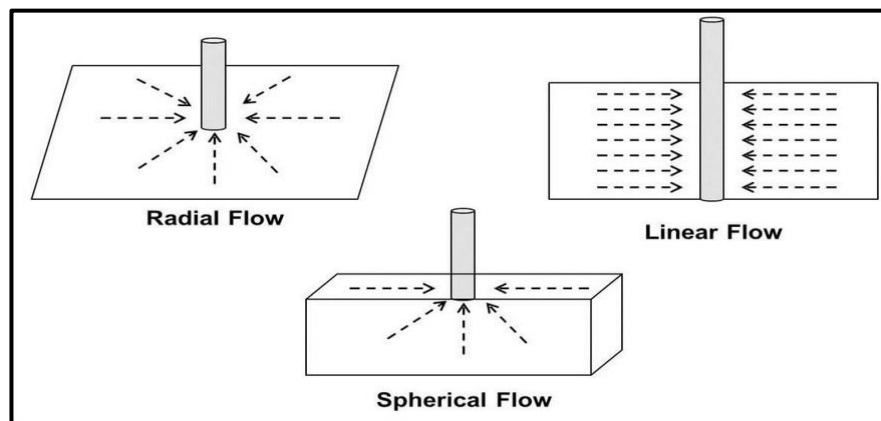


Figure I-7: flow geometries types [4].

#### I.2.3.1 Linear flow

Linear flow is common reservoirs its occurs when flow paths are parallel and the fluid flows in a single direction. The general equation that models the linear flow is (Eq I-17):

$$q = \frac{0.001127K A (p_1 - p_2)}{\mu L} \quad \text{I-17}$$

Where

- q**: flow rate, bbl/day.
- k**: absolute permeability, md.
- p**: pressure, psia.
- μ**: viscosity, cp.
- L**: distance, ft.
- A**: cross-sectional area, ft<sup>2</sup>.

### I.2.3.2 Radial flow

Radial flow it's when fluids move toward the well from all directions and coverage at the wellbore (Eq I-18).

$$Q = \frac{0.00708 k h (p_2 - p_1)}{\mu B \ln \left( \frac{r_2}{r_1} \right)} \quad \text{I-18}$$

Where

- Q**: flow rate, bbl/day.
- p<sub>2</sub>**: external pressure, psia.
- p<sub>1</sub>**: bottom-hole flowing pressure, psia.
- k**: permeability, md.
- μ**: viscosity, cp.
- B**: formation volume factor bbl/stb.
- h**: thickness, ft.
- r<sub>2</sub>**: external or drainage radius, ft.
- r<sub>1</sub>**: wellbore radius, ft.

### I.2.3.3 Spherical flow

It is possible to have a spherical or hemispherical flow near the wellbore, depending on the type of wellbore completion configuration. A well with a limited perforated interval could result in spherical flow in the vicinity of the perforations. The radial flow equation is commonly used to estimate production rates and pressure behavior [4].

### I.2.4 Basic PVT parameters

The Pressure -Volume -Temperature are parameters measured by laboratory analysis of crude oil samples. The parameters can be used to express the relationship between surface and reservoir hydrocarbon volumes. PVT analysis also provides fluid physical properties required for well test analysis and fluid flow simulation.

**The solution (or dissolved) gas oil ratio (Rs):** which is the number of standard cubic feet of gas that will dissolve in one stock tank barrel of oil when both are taken down to the reservoir at the prevailing reservoir pressure and temperature (Eq I-19).

$$R_s = \frac{(Q_g)_{p,T}}{(Q_o)_{p,T}} \quad \text{I-19}$$

Where

**Rs:** is the solution gas-oil ratio.

**Qg:** is the rate of gas production (standard cubic feet per day or cubic meters per day).

**Qo:** is the rate of oil production (barrels per day or cubic meters per day).

**The oil formation volume factor (Bo):** is the volume in barrels occupied in the reservoir, at the prevailing pressure and temperature, by one stock tank barrel of oil plus its dissolved gas (Eq I-20).

$$B_o = \frac{(V_o)_{p,T}}{(V_o)_{sc}} \quad \text{I-20}$$

Where

**Bo:** is the oil formation volume factor, res. bbl/STB.

**(Vo)P,T:** is the volume of oil at reservoir pressure and temperature (also includes gas in solution), bbl.

**(Vo)sc:** is the volume of oil at standard conditions, stock tank barrel (STB, always reported at standard conditions).

**The gas formation volume factor (Bg):** is the volume in barrels that one standard cubic foot of gas will occupy as free gas in the reservoir at the prevailing reservoir pressure and temperature (Eq I-21) [10].

$$B_g = \frac{(V)_{p,T}}{(V)_{sc}} \quad \text{I-21}$$

Where

**Bg:** is the gas formation volume factor, ft<sup>3</sup>/scf.

**(V)P,T:** is the volume of gas at reservoir pressure and temperature, ft<sup>3</sup>.

**(V)sc:** is the volume of gas at standard conditions, scf.

### I.2.5 Well Testing

Tests on oil and gas wells are performed at various stages of drilling, completion and production. The test objectives at each stage range from simple identification of produced fluids and determination of reservoir deliverability to the characterization of complex reservoir features. Most well tests can be grouped either as productivity testing or as descriptive/reservoir testing. Productivity well tests are conducted to:

- Identify produced fluids and determine their respective volume ratios.
- Measure reservoir pressure and temperature.
- Obtain samples suitable for PVT analysis.
- Determine well deliverability.
- Evaluate completion efficiency.
- Characterize well damage.
- Evaluate workover or stimulation treatment.

Descriptive tests seek to:

- Evaluate reservoir parameters.
- Characterize reservoir heterogeneities.
- Assess reservoir extent and geometry.
- Determine hydraulic communication between wells [11].

#### **I.2.5.1 The transient pressure curve analysis**

The transient pressure curve refers to the plot of pressure response over time during a well test. It shows the dynamic changes in pressure within the reservoir as a result of disruptions or changes in the flow conditions.

Pressure transient curve analysis probably provides more information about reservoir characteristics than any other technique. Horizontal and vertical permeability, well damage, fracture length, storativity ratio and interporosity flow coefficient are just a few of the characteristics that can be determined. In addition, pressure transient curves can indicate the reservoir's extent and boundary details. The shape of the curve, however, is also affected by the reservoir's production history. Each change in production rate generates a new pressure transient that passes into the reservoir and merges with previous pressure effects. The observed pressures at the wellbore will be a result of the superposition of all these pressure changes [12].

#### **I.2.5.2 Types of well test**

Different types of well tests can be achieved by altering production rates. Whereas a build-up test is performed by closing a valve (shut-in) on a producing well, a drawdown test is performed by putting a well into production. Other well tests, such as multi-rate, isochronal and injection well falloff are also possible [11].

# *Chapter II*

## *Drive mechanisms and well performance*



## II.1 Drive mechanisms

A drive mechanism refers to the natural forces that move oil and gas through a reservoir toward the production wells. These mechanisms include:

### II.1.1 Natural water drive

Natural water drive is a reservoir drive mechanism where water from an adjacent aquifer moves into the reservoir to replace the oil or gas as it is produced. This water influx helps to maintain reservoir pressure and supports the continuous flow of hydrocarbons to the wellbore. This drive mechanism can significantly enhance oil recovery, often resulting in higher recovery rates compared to other drive mechanisms [13].

### II.1.2 Solution gas drive

Solution gas drive is a reservoir drive mechanism where the primary energy for moving and producing reservoir fluids is provided by gas that is initially dissolved in the oil. As the reservoir pressure declines due to production, this dissolved gas comes out of solution, expanding and helping to push the oil towards the wellbore and up to the surface, this process typically becomes significant once the reservoir pressure falls below the bubble point, which is the pressure at which gas begins to separate from the oil. Solution gas drive can result in an oil recovery rate of about 15-20% of the original oil in place (OOIP) [14].

### II.1.3 Gas-cap drive

A gas cap drive is a reservoir drive mechanism where the primary source of energy for hydrocarbon production comes from the expansion of a gas cap located above the oil zone. As the reservoir pressure declines due to oil production, the gas cap expands, helping to displace oil towards the production wells. This mechanism helps maintain reservoir pressure and prolong oil production, resulting in typically higher recovery rates compared to solution gas drive reservoirs [15].

### II.1.4 Compaction drive

This drive mechanism might occur during depletion when rock grains are subjected to stress beyond elasticity limit. It leads to a re-compaction of partially deformed or even destroyed rock grains that might result in gradual or abrupt reduction of the reservoir pore volume [15].

## II.2 Well performance

### II.2.1 Inflow performance relationship

The Inflow Performance Relationship (IPR) describes pressure drawdown as a function of production rate, where drawdown is defined as the difference between static and flowing

bottom hole pressure (FBHP). The simplest approach to describe the inflow performance of oil wells is the use of the productivity index (PI) concept. It was developed using the following assumptions:

- Flow is radial around the well.
- A single-phase liquid is flowing.
- Permeability distribution in the formation is homogeneous.
- The formation is fully saturated with the given liquid [16].

The flow through a porous media is given by the Darcy equation (Eq II-1, EqII-2):

$$\frac{q}{A} = \frac{k}{\mu} \frac{\partial p}{\partial l} \quad \text{II-1}$$

$$q = \frac{0.00708kh}{\mu\beta\ln\left(\frac{r_e}{r_w}\right)} (P_R - P_{wf}) \quad \text{II-2}$$

Where

**q**: liquid rate, STB/d.

**k**: effective permeability, md.

**h**: pay thickness, ft.

**$\mu$** : liquid viscosity, cp.

**B**: liquid volume factor, bbl/STB.

**$r_e$** : drainage radius of well, ft.

**$r_w$** : radius of wellbore, ft.

**$p_R$** : average reservoir pressure.

**$p_{wf}$** : flowing bottomhole pressure.

Most parameters on the right hand side are constant, which permits collecting them into a single coefficient called PI:

$$q = PI(p_R - p_{wf}) \quad \text{II-3}$$

This gives

$$PI = \frac{q}{(p_R - p_{wf})} \quad \text{II-4}$$

These equations (Eq II-3 and Eq II-4) state that liquid inflow into a well is directly proportional to the pressure drawdown. It will be plotted as a straight line on a pressure versus rate diagram. The use of the PI concept is quite straightforward. If the average reservoir pressure and the PI are known, the use of (Eq II-3) gives the flow rate for any FBHP. The well's PI can either be calculated from reservoir parameters, or measured by taking flow rates at various FBHPs. This works well for a single phase flow, but when producing a multiphase reservoir the curve will not plot as a straight line. As the oil approaches the well bore and the pressure drops

below the bubble point, gas comes out of solution. Thus, the free gas saturation in the vicinity of the oil steadily increases, which implies that the relative permeability to gas steadily increases at the expense of the relative permeability of oil. The greater the drawdown, the bigger this effect would be. Since the PI depends on the effective oil permeability, it is expected that it will decrease. Figure II-1 shows the IPR curve for this condition [17].

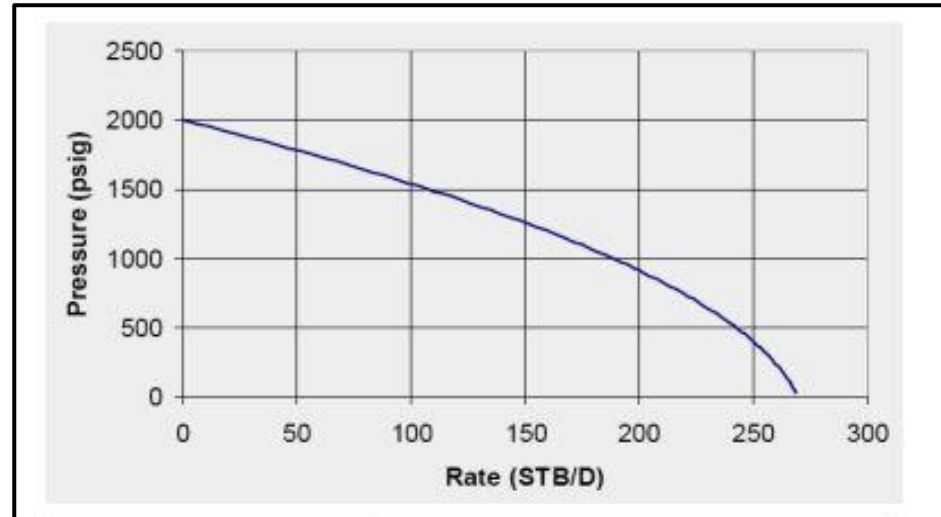


**Figure II-1: IPR typical curve [18].**

Vogel used a numerical reservoir simulator to study the inflow of wells depleting solution gas drive reservoirs. He considered cases below the bubble point and varied parameters like draw downs, fluid and rock properties. Vogel found that the calculated IPR curves exhibited the same general shape, which is given by the dimensionless equation (Eq II-5):

$$\frac{q}{q_{max}} = 1 - 0.2 \frac{P_{wf}}{2} - 0.8 \left( \frac{P_{wf}}{P_R} \right)^2 \quad \text{II-5}$$

The equation is generally accepted for other drive mechanisms as well, and is found to give reliable results for almost any well with a bottom hole pressure below the bubble point of the oil. There are a number of other models designed for special cases e.g. horizontal wells, transient flow, fractured wells, non-Darcy pressure loss, high rates, etc. [16].

### II.2.2 Outflow performance

The well's outflow performance, or Vertical Lift Performance (VLP), describes the bottomhole pressure as a function of flow rates. The outflow performance is dependent on different factors; liquid rate, fluid type (gas to liquid ratio, water cut), fluid properties, and tubing size. Gabor divides the total pressure drop in a well into a hydrostatic component, a friction component, and an acceleration component: The hydrostatic component represents the change in potential energy due to gravitational force acting on the mixture.

$$\left( \frac{dp}{dl} \right)_h = \rho g \sin \beta \quad \text{II-6}$$

Where

$\rho$ : density of fluid.

$\beta$ : pipe inclination angle, measured from horizontal.

$g$ : gravity constant.

The friction component (Eq II-7) stands for the irreversible pressure losses occurring in the pipe due to fluid friction on the pipe's inner wall:

$$\left(\frac{dp}{dl}\right)_f = \frac{1}{d} f \frac{1}{2} \rho v^2 \quad \text{II-7}$$

Where

$f$ : friction factor.

$d$ : pipe inside diameter.

$v$ : fluid velocity.

The type of flow is determined from the Reynolds number:

$$R_e = \frac{\rho v d}{\mu} \quad \text{II-8}$$

The boundaries between flow regimes are:

$Re \leq 2000$ : Laminar flow.

$2000 < Re \leq 4000$ : Transition between laminar and turbulent flow.

$4000 < Re$ : Turbulent flow.

For laminar flow  $f = 64/Re$  (Moody friction factor). However, finding the friction factor is more complicated for turbulent flow, and there are several ways to calculate the friction factor.

The acceleration component represents the kinetic energy changes of the flowing mixture and is proportional to the changes in flow velocity. The term is often negligible:

$$\left(\frac{dp}{dl}\right)_a = -\rho v \frac{dv}{dl} \quad \text{II-9}$$

### II.2.2.1 Other Effects

#### II.2.2.1.1 Effect of liquid flow rate on pressure loss

From the friction equation, we can see that friction losses increase as liquid rate increases ( $v$  increases). The

hydrostatic gradient also increases with increased liquid production.

#### II.2.2.1.2 Effect of gas-to-liquid ratio on pressure loss

An increase in gas-to-liquid ratio (GLR) results in a reduction of the hydrostatic gradient. On the other hand, increased GLR increases friction forces and has a counter effect on the

bottomhole pressure. When the contribution of the friction becomes higher than that of hydrostatic forces, the actual bottomhole pressure starts to increase. From a gas lift point of view, this means that there is a limit of how much gas that beneficially can be injected.

#### II.2.2.1.3 Effect of water cut on pressure loss

Increased water cuts result in increased liquid density, which in turn, increases hydrostatic forces and the bottomhole pressure

#### II.2.2.1.4 Effect of tubing size on pressure loss

From the equation II-7, we can see that the increased tubing diameter reduces the pressure gradient due to friction. However, there is a limit to which the tubing diameter can be increased. If the diameter is too big the velocity of the mixture ( $v=q/A$ , A: pipe cross section) is not enough to lift the liquid and the well starts to load up with liquid, resulting in increase of hydrostatic pressure.

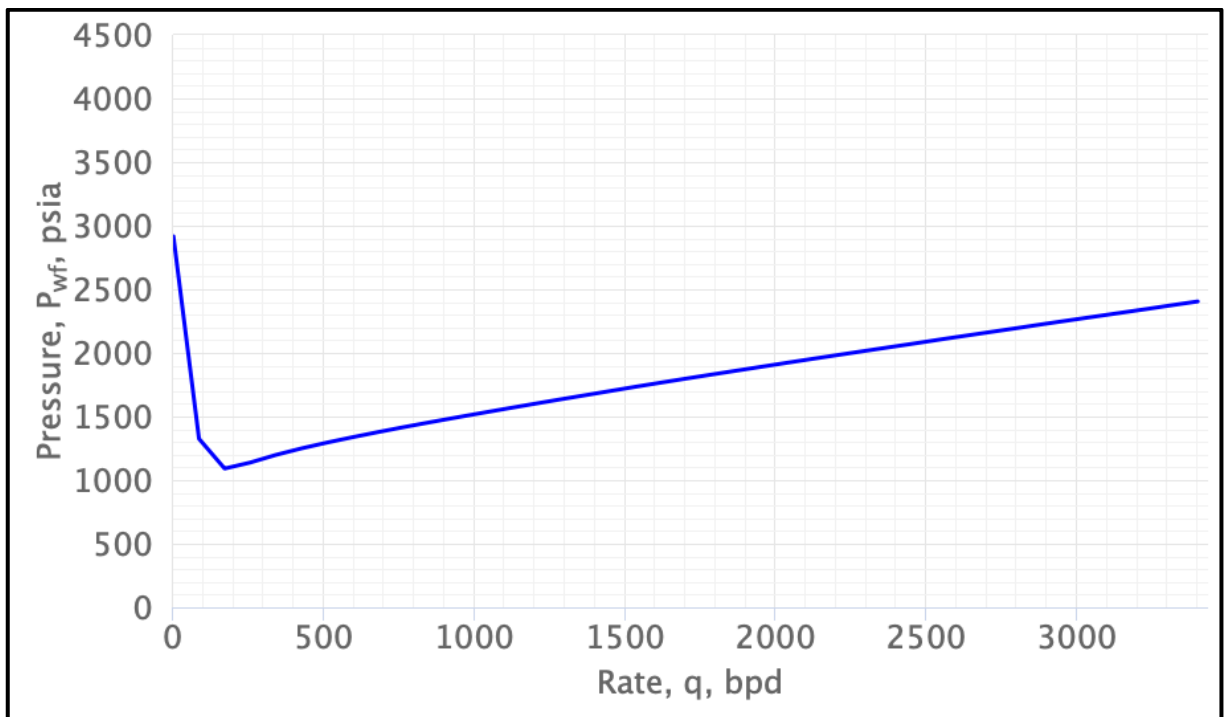
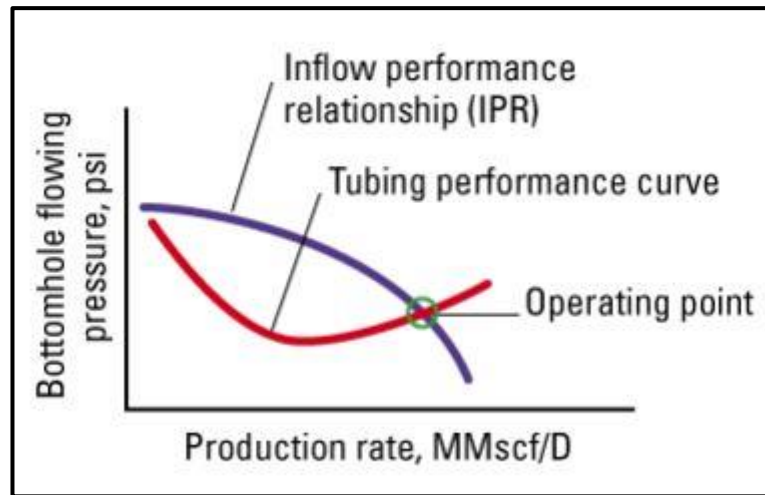


Figure II-2: VLP typical curve [19].

### II.2.3 Operating point

To calculate the well production rate, the bottom-hole pressure that simultaneously satisfies both the IPR and VLP relations is required. By plotting the IPR and VLP in the same graph the producing rate can be found. The system can be described by an energy balance expression, simply the principle of conservation of energy over an incremental length element of tubing. The energy entering the system by the flowing fluid must equal the energy leaving the system plus the energy exchanged between the fluid and its surroundings.



**Figure II-3:** Operating point (intersection between IPR and VLP curves) [20].

### II.3 Artificial lift

During the production life of a reservoir, its pressure will decline. The fluid column weight increases due to the increased density of the water and oil mixture, resulting in higher hydrostatic pressure. In this scenario, the reservoir pressure may not be sufficient to lift the fluid from the bottom to the surface. This pressure decline can significantly reduce, or even halt, fluid flow from the well (Figure II-4). To counteract this, artificial lift techniques are employed to add energy to the produced fluids, thereby increasing production rates by reducing down-hole pressure and enhancing drawdown (Figure II-5). In addition, for the fact that artificial lift installed in wells increases the production rate, there are some problems encountered after the installation of these lifting techniques. Such as solid/sand handling ability, corrosion/scale handling ability, water coning, high water cut, the stability, number of wells, flowing pressure and temperature limitation, well depth, production rate, flexibility, high GOR, electrical power, space, economics etc. which are factors to consider in the selection prior to the installation of any of the artificial lift techniques [21].

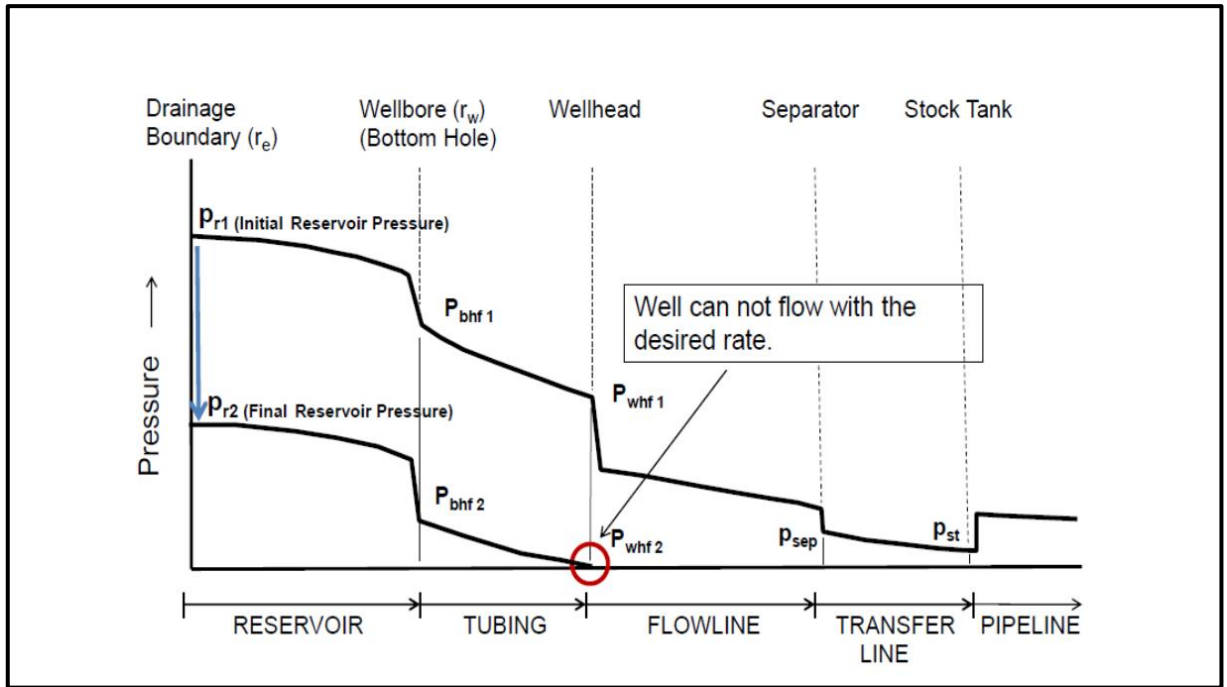


Figure II-4: Schematic Pressure Profile for Production System (natural flow) [20].

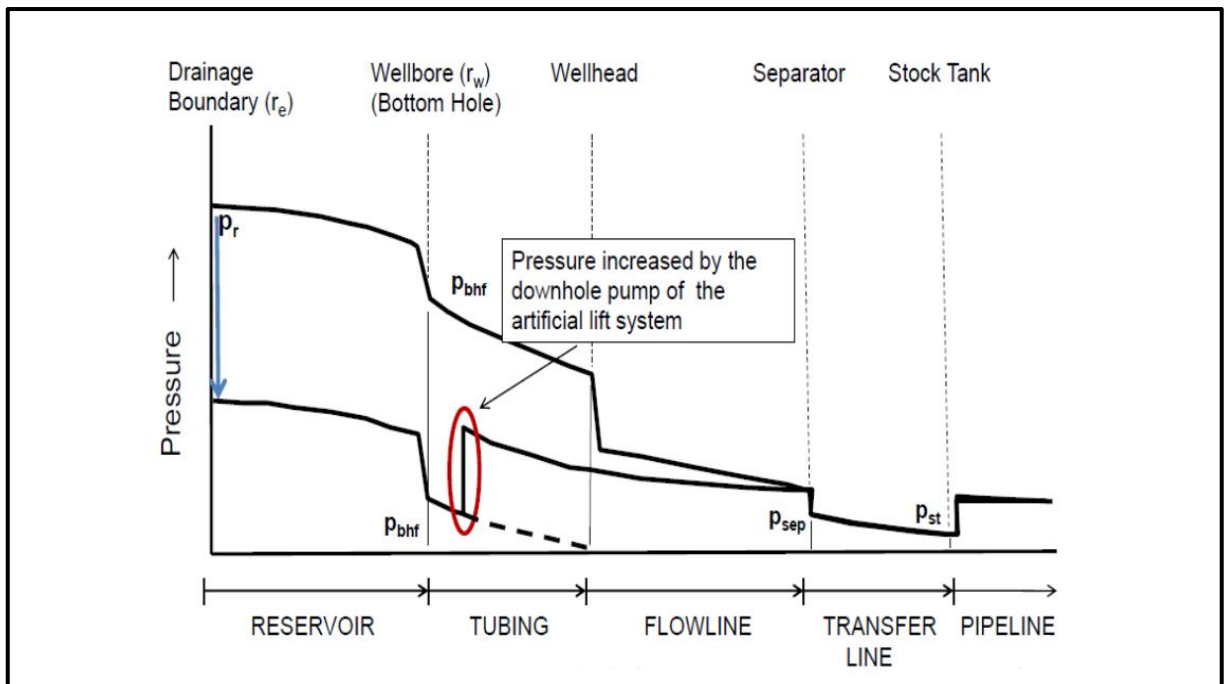


Figure II-5: Schematic Pressure Profile for Production System (artificial lift) [22].

Artificial lift methods fall into two groups, those that use pumps and those that use gas.

#### Pump Types:

- Beam Pump / Sucker Rod Pumps (Rod Lift).
- Progressive Cavity Pumps (Jet /piston lift).
- Subsurface Hydraulic Pumps.
- Electric Submersible Pumps (ESP).



**Gas Method:**

- Gas Lift.

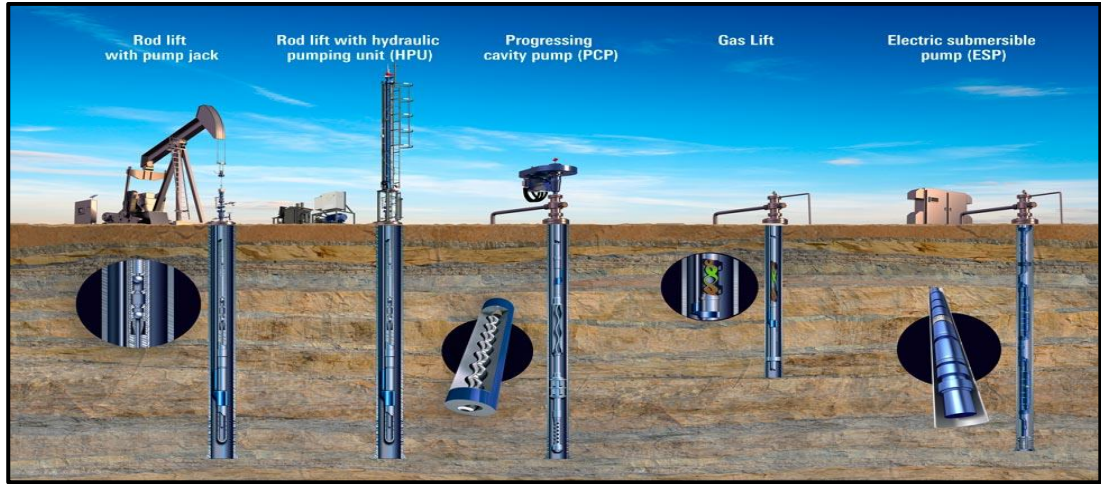


**Figure II-6:** Artificial lift method [23].

### II.3.1 Electrical Submersible Pumps

The Electrical Submersible Pump (ESP) is an artificial lift method widely used in oil production, especially for offshore operations. Currently, more than 150,000 oil wells are operated worldwide with ESP. A schematic view of ESP is presented in (Figure II-7).

Electrical Submersible Pumps are divided into two parts: surface components and subsurface components.

**Surface components:**

- Motor controller.
- Transformer.
- Surface electric cable.

**Subsurface components:**

- Pump.
- Motor.
- Seal section.
- Gas separator [24].



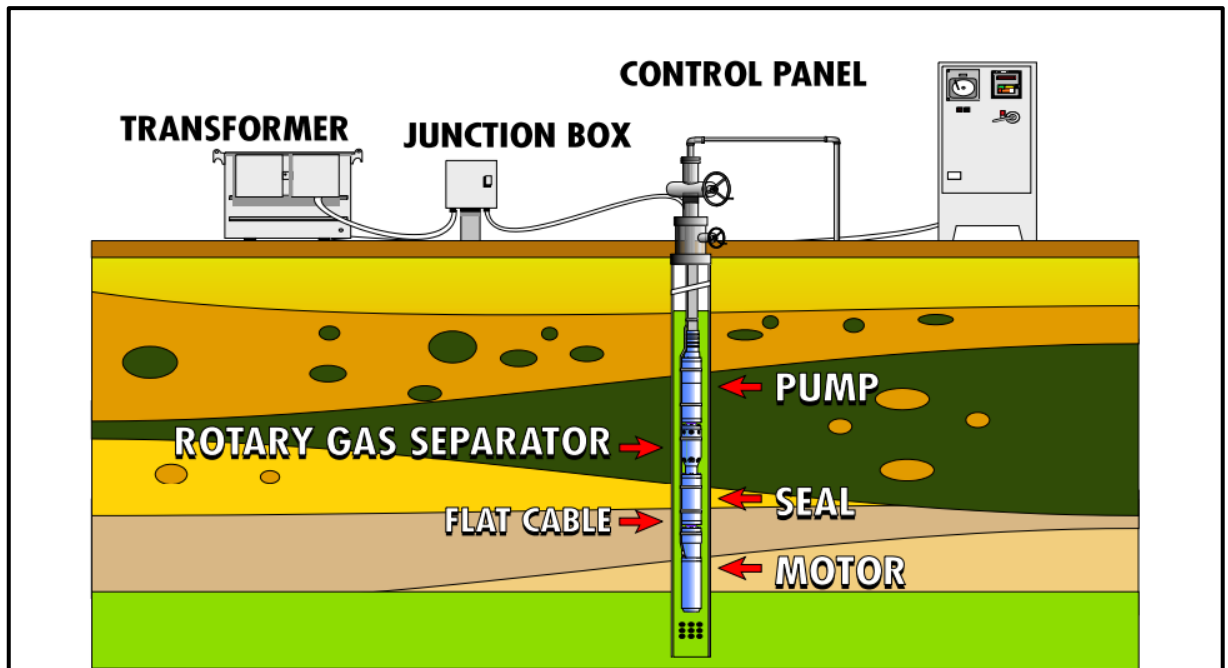


Figure II-7: Schematic view of ESP [25].

### II.3.1.1 Electrical Submersible Pumps lifting mechanism

An Electrical Submersible Pump (ESP) is a multistage centrifugal pump with stages determined by well requirements and completion design. Each stage has a rotating impeller and stationary diffusers, typically made from high-nickel iron to resist abrasion and corrosion. Fluid enters the first stage, passes through the impeller where it gains velocity, and then through the diffuser where the velocity is converted to pressure. This process repeats through each stage, incrementally increasing the fluid's pressure until it reaches the total developed head necessary to reach the surface.

The ESP is driven by an induction motor that can exceed 5,000 rpm with a variable speed drive. The pump's performance is illustrated by a performance curve that shows the relationship between horsepower, efficiency, flow rate, and head relative to the operating flow rate. Each pump's catalog performance curve defines its recommended operating range. By monitoring these parameters over time, operators can determine when the ESP falls out of its optimal range and decide whether to resize the pump or replace it to match the actual flow rate [11].

### II.3.1.2 Advantages and Disadvantages of Electrical Submersible Pumps

Table II-1: Advantages and disadvantages of the ESP [23].

Advantages	Disadvantages
High energy addition	Limited sand tolerance

High production rates	Run lives limited if poorly designed, installed, operated
High efficiency (70%)	Low GLR tolerance (without separator)
Unaffected by deviation	Rig or hoist required on failure
Good data gathering tie-in	Electrical (cable) failures
Easily controlled	Limited temperature tolerance

### II.3.2 Gas lift

Gas lift is a widely used method in offshore and onshore fields, due to its very simple design and it has very few moving parts. Gas lift method is applicable in highly deviated, high GOR wells and fluids with high sand content. Gas lift is an artificial lift method that closely resembles the natural flow process, requiring primarily a supply of pressurized injection gas. Typically, the lift gas is sourced from other producing wells, separated from the oil, compressed, and injected into the annulus at high pressure. The gas from the producing well is then recovered, recompressed, and re-injected. However, the gas compression process is energy-intensive and costly. A schematic view of Gas Lift method is presented in Figure II-8 [26].

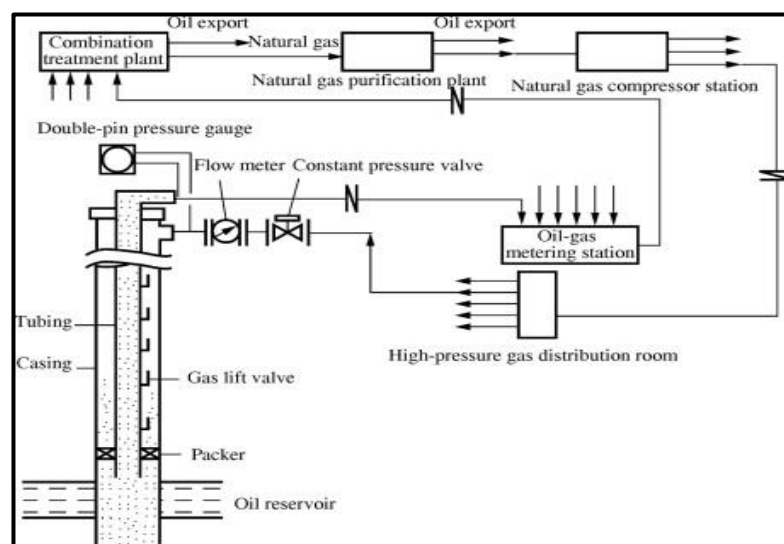


**Figure II-8:** Schematic view of GL method [27].

The main parts of gas lift system are:

- Station for gas compression.
- Injection manifold.
- Injection chokes.

- d) Surface controllers.
- e) Injection valves and chamber that are installed in down-hole.

### II.3.2.1 Gas lift mechanism

In the gas lift method, production is increased by reducing bottomhole pressure through the injection of compressed gas into the annulus or through an orifice installed in the tubing. This gas impacts the liquid in two ways:

- a) It causes expansion in the liquid phase, moving oil to the surface.
- b) It decreases the density of the oil, reducing hydrostatic pressure and aiding in lifting the oil to the surface.

The gas lift method can be applied to four types of wells:

1. High bottomhole pressure (BHP) and high productivity index (PI) wells.
2. Low BHP and high PI wells.
3. High BHP and low PI wells.
4. Low BHP and low PI wells.

The gas lift process can be summarized in four steps:

1. Injection of the compressed gas into the annulus or through gas lift valves.
2. Lifting of reservoir fluids to the surface by the injected gas.
3. Separation of gas and liquid in the separator, with the gas either being recompressed or transported to sales manifolds.
4. Compression of gas at the surface and transportation to the designated wells [28].

### II.3.2.2 Advantages and Disadvantages of Gas Lift method

**Table II-2:** Advantages and disadvantages of the gas lift method [23].

Advantages	Disadvantages
Reliable operation	Inefficiency in low volume systems due to compression and gas treatment capital costs
High tolerance to solids (though erosional velocities in tubing and Xmas tree may be critical)	Requirement for start-up gas to kick-off
Ability to handle high production rates	Difficulty with very heavy/viscous crude
Usefulness in offshore operations where space for pump systems may be limited	Potential for hydrate problems on surface or in the GLVs

Generally maintainable with wireline	Requirement for continuous monitoring, optimization and trouble shooting. (This is not straightforward but essential)
Full-bore, through-tubing access to below gas lift valves	Limitation often imposed by restricted maximum lifting depth (governed by minimum FBHP)

# *Chapter III*

## *Water coning and its remedial techniques*

### III.1 Water coning

The production of water from oil producing wells is a common occurrence in oil fields, which results from one or more reasons such as the normal rise of water oil contact, water coning, and water fingering. We will deal with one cause of this water production, namely, coning. Coning is a fundamental petroleum engineering problem since oil is very often found below a gas zone, above a water zone, or sandwiched between these two zones. In general, coning is the term used to describe the mechanism underlying the upward movement of water into the producing well [4].

Water coning may lead to several serious problems. For example, the water is usually corrosive and its disposal cost is high. The affected well can be abandoned early. Moreover, there may be a loss in total recovery [29].

### III.2 The physics of water coning

Water coning in oil wells is primarily influenced by pressure drawdown and fluid movement. Pressure drawdown near the wellbore creates a substantial pressure gradient, while reservoir fluids move towards the zone of least resistance, contributing to coning (Figure III-1). Capillary forces have a negligible impact, while viscous forces, related to fluid flow through the reservoir, and gravity forces, acting in the vertical direction due to density differences, play significant roles. At any time, there is an equilibrium between viscous and gravity forces. When viscous forces exceed gravitational ones, the cone breaks into the well. However, if gravity forces exceed viscous forces at steady-state conditions, a stable water cone forms and does not reach the well. In unsteady-state conditions, the cone moves towards the well until a steady-state condition is reached. If the flowing pressure drop is sufficient, the unstable cone expands and eventually breaks into the well. The instability of the water cone is due to the high upward dynamic force, causing water to flow upward and break through into the wellbore [2].

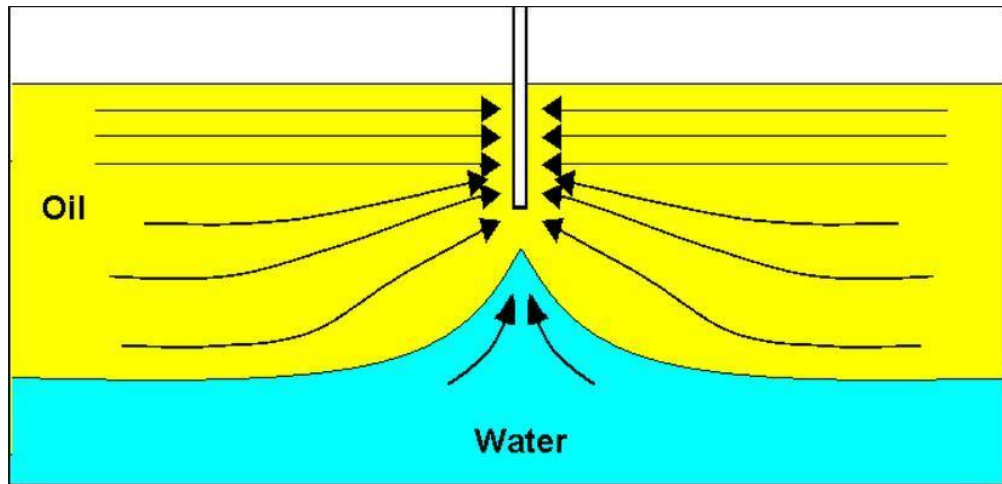


**Figure III-1:** water coning in vertical wells [29].

### III.3 Water control diagnostics plots

According to Chan (1995), the log-log plots of Water-Oil Ratio (WOR) versus time show different characteristic trends for different mechanisms. The time derivative of WOR is found to be capable of differentiating whether the well is experiencing: water coning, high permeability layer breakthrough or near wellbore channelling. WOR and WOR' can be calculated using the equations below (Eq III-1, Eq III-2).

$$WOR = \frac{Q_w}{Q_o} \quad \text{III-1}$$

$$WOR' = \frac{WOR_2 - WOR_1}{t_2 - t_1} \quad \text{III-2}$$

Chan identified three most noticeable water production mechanisms namely water coning, near well-bore problems and multi-layer channelling. Log-log plots of the WOR (rather than water cut) versus time were found to be more effective in identifying the production trends and problem mechanisms. It was discovered that derivatives of the WOR versus time can be used for differentiating whether the excessive water production problem as seen in a well is due to water coning or multilayer channelling. Log-log plots of WOR and WOR' versus time for the different excessive water production mechanisms are shown in (Figures III-2 to III-4).

Chan (1995) proposed that the WOR derivatives can distinguish between coning and channelling. Channelling WOR' curves should show an almost constant positive slope (Figure III-2).

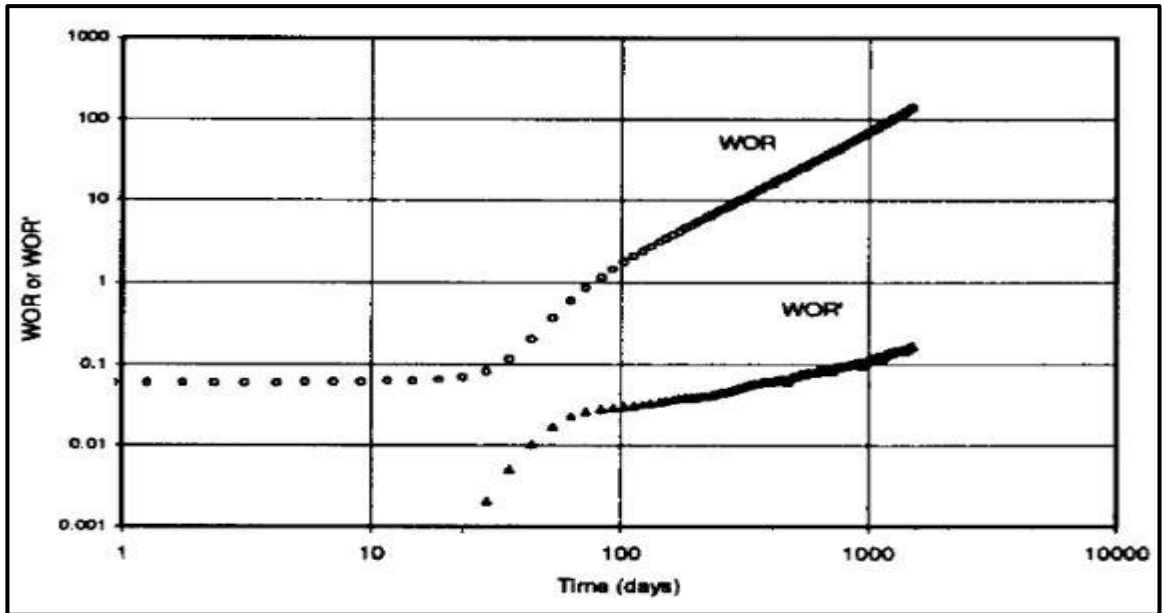


**Figure III-2:** Multi-layer channelling WOR and WOR derivatives [31].

As opposed to coning WOR' curves, this should show a changing negative slope (Figure III-3).

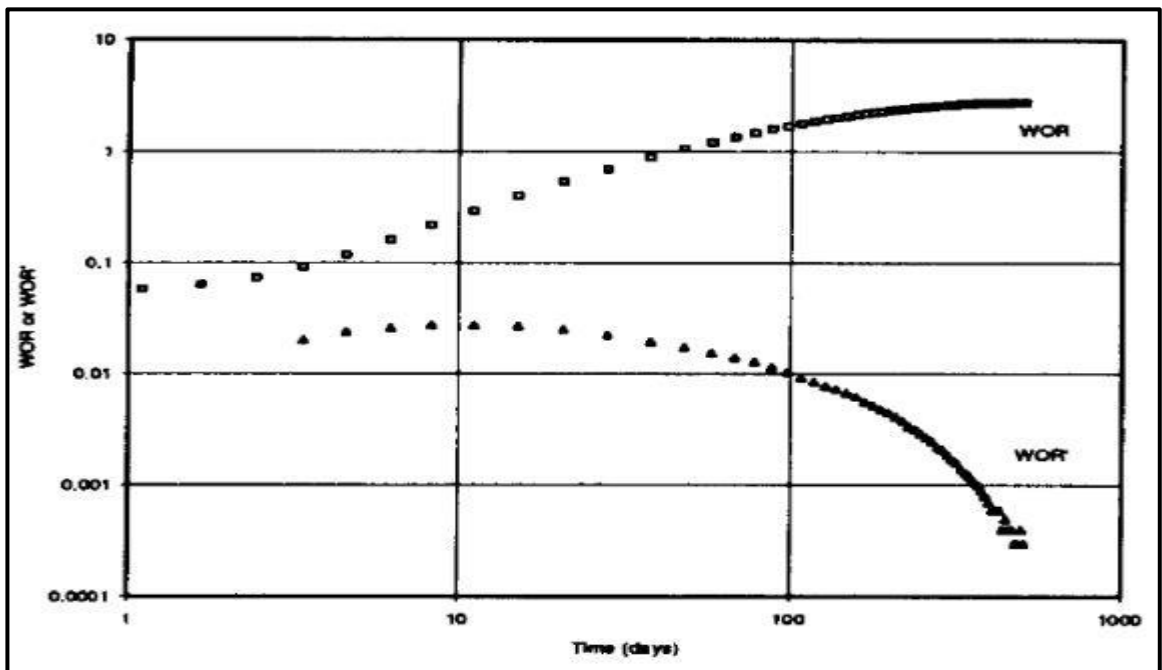


**Figure III-3:** Bottom-water coning WOR and WOR derivatives [31].

A negative slope turning positive when “channelling” occurs as shown in (Figure III-4), characterizes a combination of the two mechanisms. Chan classifies this as coning with late channelling behaviour [31].



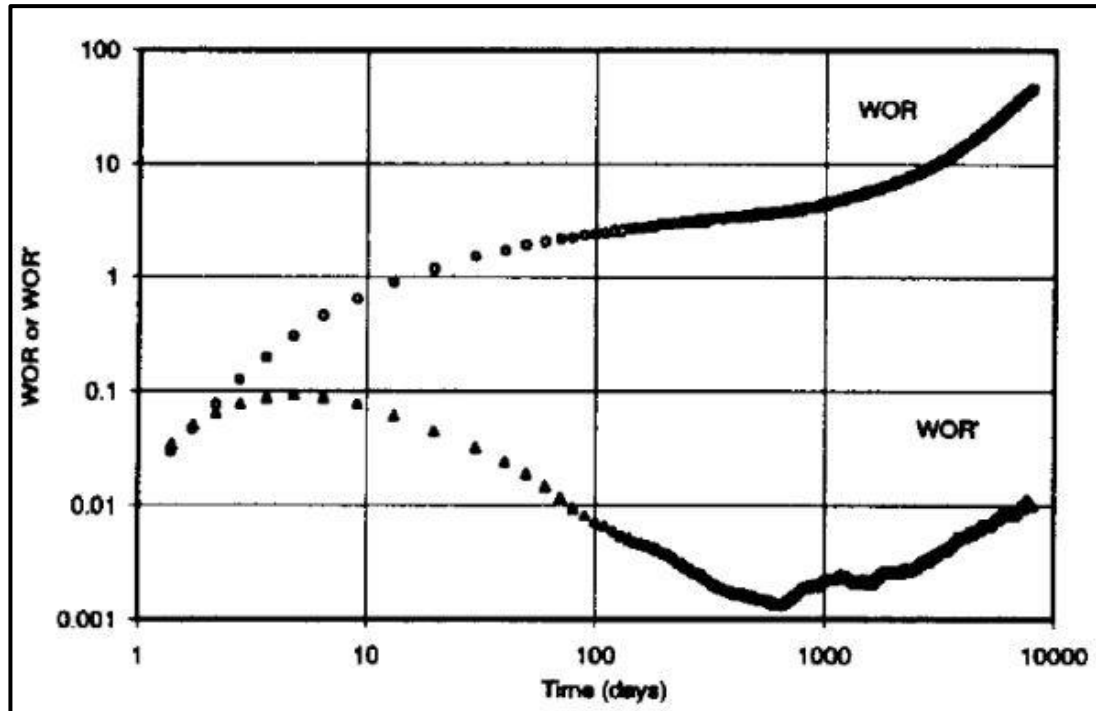


Figure III-4: Bottom water coning with late time channelling [31].

### III.4 Prediction of water coning

Several studies have been performed to predict and mitigate water coning in the production of oil and gas. The early study of water coning phenomenon was based on the understanding of well and coning configurations. Several authors have developed correlations to predict coning problem in terms of critical oil rate; that is, the maximum production oil rate without producing water, water breakthrough time, and water-oil ratio (WOR) after breakthrough. Generally, these correlations formulation can be divided into two categories, the first category determines the correlations analytically based on the equilibrium conditions of viscous and gravity forces in the reservoir, while the second category is based on empirical correlations developed from laboratory experiments or computer simulation.

#### III.4.1 Calculation of critical oil rate

##### III.4.1.1 The Meyer and Garder correlation

Meyer and Garder (1954) analytically determined the maximum critical flow of oil into a well without the water zone coning into the production section of the well. In order to simplify the analytical treatment, a homogeneous reservoir and radial flow were assumed. Meyer and Garder derived the following equation (Eq III-3) for critical rate calculation [4].

$$Q_{oc} = 0.246 \times 10^{-4} \left[ \frac{\rho_w - \rho_o}{\ln(r_e/r_w)} \right] \left( \frac{k_o}{\mu_o B_o} \right) (h^2 - h_p^2) \quad \text{III-3}$$

Where

**Q<sub>oc</sub>**: critical oil rate, STB/day.

$\rho_w$ : water density, lb/ft<sup>3</sup>.

$\rho_g$ : density of gas, lb/ft<sup>3</sup>.

$\mu_o$ : oil viscosity, cp.

$B_o$ : oil formation volume factor, bbl/STB.

$h$ : oil column thickness, ft.

$h_p$ : perforated interval, ft     $h_p = h - D_t$ .

$k_o$ : effective oil permeability, md.

$r_e, r_w$ : drainage and wellbore radius, respectively, ft.

#### III.4.1.2 The Chaney et al method

This method is an extension of Muskat's method. The method is based upon the results of mathematical and potentiometric analyses of water coning.

Chaney's curves show critical production rates in reservoir barrels per day versus the distance from the top of the perforated interval to the top of the sand. Curves are shown for sand thicknesses of 12.5, 25, 50, 75, and 100 feet; all having drainage radius of 1,000 feet, Chaney's data were least square fitted. The following equation (Eq III-4, Eq III-5) was obtained and can be used for prediction with a programmable calculator:

$$q_{\text{curve}} = 0.1313(h^2 - d^2) - 23.2 \quad \text{III-4}$$

Where

$q_{\text{curve}}$ : critical production rate from Chaney's curves, (RB/D).

The critical production rates from Chaney's curves were developed using the following fluid and rock characteristics:

Permeability ( $k$ ) = 1,000 md.

Oil Viscosity ( $\mu_o$ ) = 1 cp.

Density difference between water and oil ( $\rho_w - \rho_o$ ) = 0.3 g/cc.

It is necessary to correct the rates obtained from Chaney's curves for the actual values of fluid and rock properties by the following equation (Eq III-5) [32].

$$Q_{OC} = \frac{0.00333 k (\rho_w - \rho_o) q_{\text{curve}}}{B_o \mu_o} \quad \text{III-5}$$

#### III.4.1.3 Hoyland-Papatzacos-Skjaeveland correlation

Hoyland, Papatzacos, and Skjaeveland (1989) presented two methods for predicting the critical oil rate for bottom water coning in anisotropic, homogeneous formations with the well completed from the top of the formation.

To predict the critical rate, the authors superimpose the same criteria as those of Muskat and Wyckoff on the single-phase solution and, therefore, neglect the influence of cone shape

on the potential distribution. Hoyland and his coworkers presented their analytical solution in the following form:

$$Q_{oc} = 0.246 \times 10^{-4} \left[ \frac{h^2(\rho_w - \rho_o)k_h}{\mu_o \beta_o} \right] Q_{CD} \quad \text{III-6}$$

Where

**Q<sub>oc</sub>**: critical oil rate, STB/day.

**h**: total thickness of the oil zone, ft.

**ρ<sub>o</sub>**: oil density, lb/ft<sup>3</sup>.

**ρ<sub>w</sub>**: water density, lb/ft<sup>3</sup>.

**k<sub>h</sub>**: horizontal permeability, md.

**Q<sub>cd</sub>**: dimensionless critical flow rate (it is correlated with the dimensionless radius  $r_D$ , and fractional well penetration ratio ( $h_p / h$ )).

**h<sub>p</sub>**: penetration interval.

**Bo**: oil formation volume factor, Bo, bbl/STB.

**μ<sub>o</sub>**: oil viscosity, cp.

The authors correlated the dimensionless critical rate  $q_{CD}$  with the dimensionless radius  $r_D$  and the fractional well penetration ratio  $h_p/h$  as shown in Figure III-5.

$$r_d = \frac{r_e}{h} \sqrt{\frac{k_v}{k_h}} \quad \text{III-7}$$

Where

**h**: total thickness of the oil zone, ft.

**k<sub>h</sub>**: horizontal permeability, md.s

**k<sub>v</sub>**: vertical permeability, md.

**r<sub>e</sub>**: radius of the reservoir, ft [4].

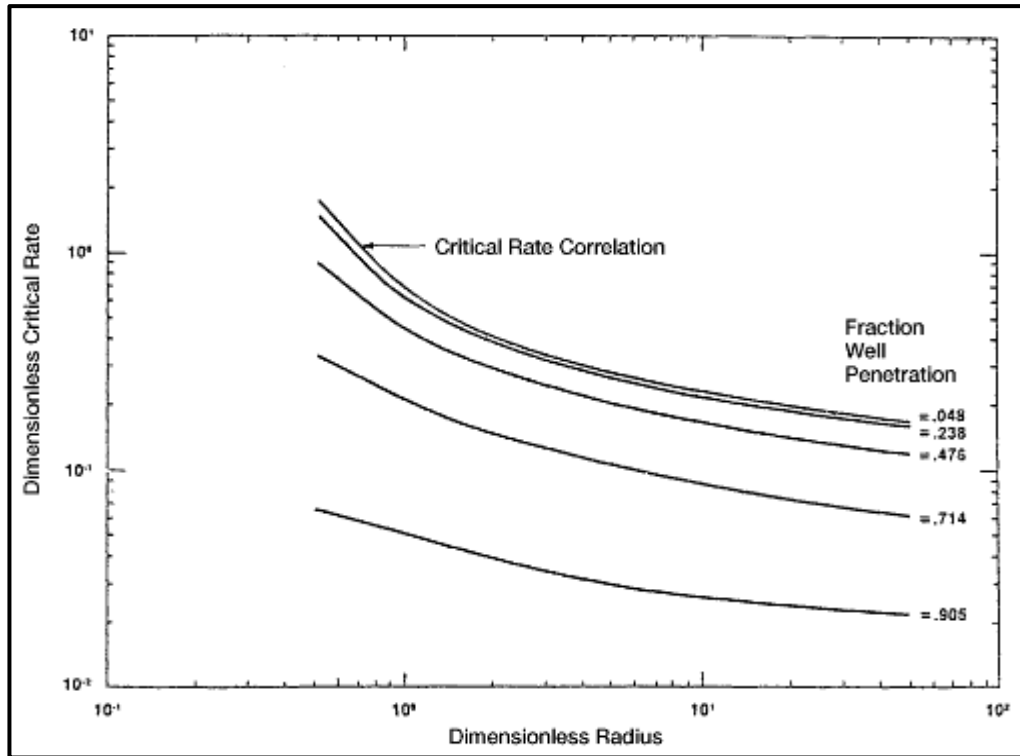


Figure III-5: Critical rate correlation [4].

#### III.4.1.4 Chaperson method

Chaperson (1986) assumes anisotropic formation. It is also assumed that the completion interval is too short. Chaperson's relationship accounts for the distance between the production well and the boundary. The relation is given in the following equation (Eq III-8):

$$Q_{co} = 0.0783 \times 10^{-4} \frac{K_h (h - h_p)^2}{\mu_o B_o} (\Delta\rho) q_c^* \quad \text{III-8}$$

Where

$Q_{co}$ : critical oil rate, STB/day.

$k_h$ : horizontal permeability, md.

$h$ : oil column thickness, ft.

$h_p$ : perforated interval, ft.

$\Delta\rho = (\rho_w - \rho_o)$ : density difference, lb/ft<sup>3</sup>.

$B_o$ : oil formation volume factor,  $B_o$ , bbl/STB.

$\mu_o$ : oil viscosity, cp [33].

Joshi (1991) correlated the coefficient  $q_c^*$  with the parameter  $\alpha'$  as:

$$\alpha' = r_e / h \sqrt{k_w / k_h} \quad \text{III-9}$$

$$q_c^* = 0.7311 + (1,9434 / \alpha') \quad \text{III-10}$$

### III.4.1.5 Schols' method

Schols (1972) developed an empirical equation based on results obtained from a numerical simulator and laboratory experiments. His critical rate equation has the following form (Eq III-11):

$$Q_c = \left( \frac{(\rho_w - \rho_o)k(h^2 - h_p^2)}{2049\mu_o\beta_o} \right) \left( 0.432 + \frac{\pi}{\ln\left(\frac{r_e}{r_w}\right)} \left(\frac{h}{r_e}\right)^{0.14} \right) \quad \text{III-11}$$

Where

**k<sub>o</sub>**: effective oil permeability, md.

**r<sub>w</sub>**: wellbore radius, ft.

**h<sub>p</sub>**: perforated interval, ft.

**ρ**: density, g/cc.

Schols' empirical formula offers a quick and good method of calculating critical rates [4].

### III.4.2 Calculation of the breakthrough time

Water breakthrough in vertical wells starts earlier than in horizontal wells. It is very important to forecast when the water in the aquifer will start to break into the production well. The most widely used correlations to predict the breakthrough time for vertical wells are by Sobocinski and Cornelius (1964), and Bournazel and Jeanson (1971).

#### III.4.2.1 The Sobocinski-Cornelius correlation

The authors correlated the breakthrough time with two dimensionless parameters: the dimensionless cone height and the dimensionless breakthrough time.

The dimensionless cone height is expressed by the equation (Eq III-12):

$$Z = 0.492 \times 10^{-4} \frac{(\rho_w - \rho_o)k_h h(h - h_p)}{\mu_o\beta_o Q_o} \quad \text{III-12}$$

Where

**ρ**: density, lb/ft<sup>3</sup>.

**k<sub>h</sub>**: horizontal permeability, md.

**Q<sub>o</sub>**: oil production rate, STB/day.

**h<sub>p</sub>**: perforated interval, ft.

**h**: oil column thickness, ft.

Dimensionless breakthrough time is calculated using this equation (Eq III-13):

$$(t_D)_{BT} = \frac{4Z + 1.75Z^2 - 0.75Z^3}{7 - 2Z} \quad \text{III-13}$$

Time to breakthrough is calculated using this equation (Eq III-14):

$$t_{BT} = \frac{20.325\mu_o h\phi(t_D)_{BT}}{(\rho_w - \rho_o)k_v(1 + M^\alpha)} \quad \text{III-14}$$

Where

$t_{BT}$ : time to breakthrough, days.

$\phi$ : porosity, fraction.

$M$ : water-oil mobility ratio and it is defined as (Eq III-15):

$$M = \frac{(K_{rw})_{sor} (\mu_o)}{(k_{ro})_{swc} (\mu_w)} \quad \text{III-15}$$

$(k_{ro})_{swc}$ : oil relative permeability at connate water saturation.

$(k_{rw})_{sor}$ : water relative permeability at residual oil saturation.

$\alpha = 0.5$  for  $M \leq 1$

$\alpha = 0.6$  for  $1 < M \leq 10$

#### III.4.2.2 The Bournazel-Jeanson Correlation

Bournazel and Jeanson (1971) developed the correlation based on experimental studies. They used the same dimensionless group as in the methodology of Sobocinski and Cornelius (1964). The steps for calculation of breakthrough time are as listed below:

- The dimensionless cone height is calculated from equation III-12.
- The dimensionless breakthrough time is calculated using equation III-16

$$(t_D)_{BT} = \frac{Z}{3-0.7Z} \quad \text{III-16}$$

- The time of breakthrough,  $t_{BT}$  is calculated using equation III-14 [4].

### III.5 Water coning control methods

Several practical solutions for water coning control methods have been developed to delay water breakthrough time and minimize the severity of water coning in oil wells. The basic methods included:

#### a) Mechanical and completion methods:

- Plugs and Packers.
- Intelligent well completions.
- Downhole oil-water separation technology.
- Downhole water sink (DWS) method and Downhole water loop (DWL) method.
- Drilling horizontal wells.
- Total penetration method.

#### b) Chemical Methods:

- Polymer flooding and Gel Injection.

### III.5.1 Mechanical and completion methods

#### III.5.1.1 Plugs and packers

One of the most well-known mechanical solutions for water shutoff and isolation operations inside the wellbore is the installation of packers and plugs. They can be installed without the drilling rig by using coiled tubing which can run them through the wellbore.

Simply, the concept of packers and plugs is a small diameter element, mainly rubber, which can expand downhole the wellbore into larger diameters, creating a seal and can be used to isolate unwanted water production zones inside the wellbore. There are different types of packers and plugs with different properties and setting techniques. Some elements expand by interacting with certain types of fluids (oil, water, or hybrid) which are known as “swellable packers”. They also depend on pre-designed properties like temperature, pressure, and salinity of the formation fluid. That can be a disadvantage in some cases and leads to failure in setting the element. If those properties are not accounted for accurately, that might lead to a faster inflation of the elements or even slower inflation than expected. In the worst cases scenario, the element might not inflate at all. Other packers and plugs inflate by applying pressure on the element in order to expand and seal. These types of plugs usually inflate by pumping darts, steel balls, or fluid to apply pressure on the rubber element and allow it to expand and increase its diameter [34].

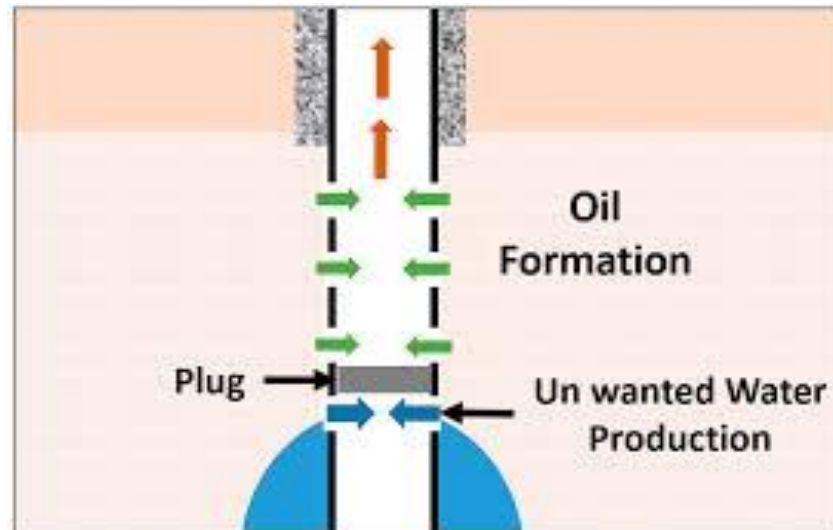


**Figure III-6:** Using plug to shut off the production of water from the bottom [34].

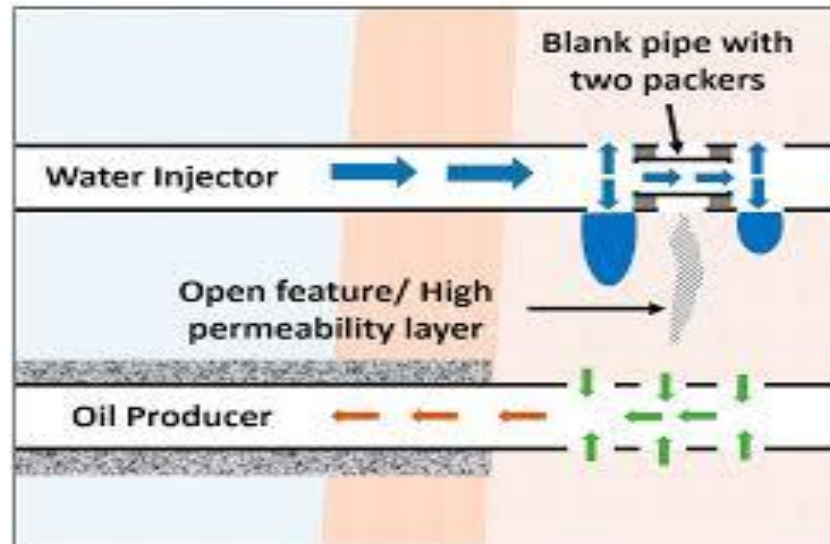


**Figure III-7:** Two packers above and below a blank pipe to shut-off water production from middle and upper part [34].

### III.5.1.2 Intelligent completions

Intelligent well completion is a revolutionary technology that enables real-time monitoring and control of well production. This system collects, transmits, and analyzes data on wellbore production, reservoir, and completion integrity, allowing for remote action to optimize reservoir control and well performance. The technology involves installing special tools and equipment, including packers, sensors, and downhole Inflow Control Valves (ICV), which enable the selection of desired production zones, control of water breakthrough, and management of water injection for pressure maintenance. Although it is a highly effective technology, its high cost, particularly the installation of ICV, can be a significant barrier. The design of the completion tool depends on various factors, including well characteristics, reservoir conditions, and water-oil contact. While intelligent well completion cannot prevent the coning phenomenon, it can effectively control its severity, making it a valuable tool in the oil field [29].



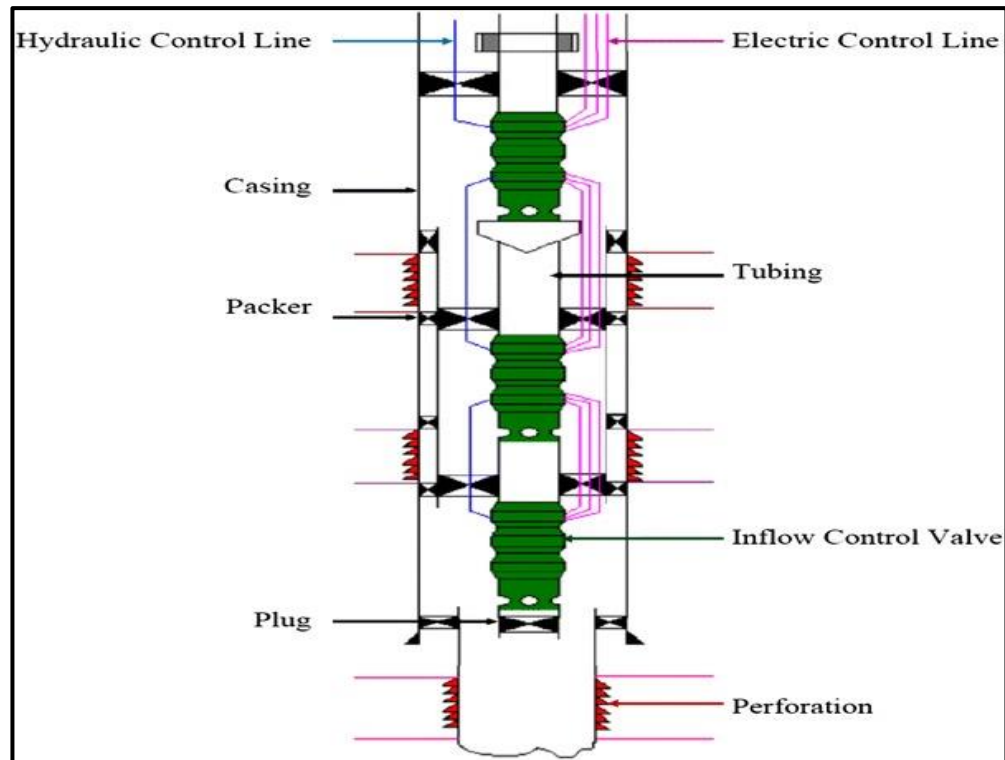


**Figure III-8:** intelligent well completion [35].

### III.5.1.3 Downhole oil-water separation

Downhole oil-water separation (DOWS) involves the use of hydrocyclone or gravitational separators and special design downhole pumps installed in the completion/production string to separate the oil and water mixture within the wellbore. Figure III-9 and figure III-10 depict a typical configuration of the downhole oil-water separation technology. This technology has been in the oil and gas industry since the 1990s, however, despite its economic and environmental advantages, only a limited number of the system has been installed in the oil and gas wells. This development is due to the complexity of the technology, as wellbore space being very limited. Thus, the separators designed (must be narrow) for the operation hindered the minimum casing size requirement. Additionally, the technology provides reduced surface water handling, but the fundamental problem of water interference with oil production within the reservoir creating bypass oil remains unresolved with this technology. Therefore, the problem of bypassed oil by the water cone development is not mitigated by this technology [29].

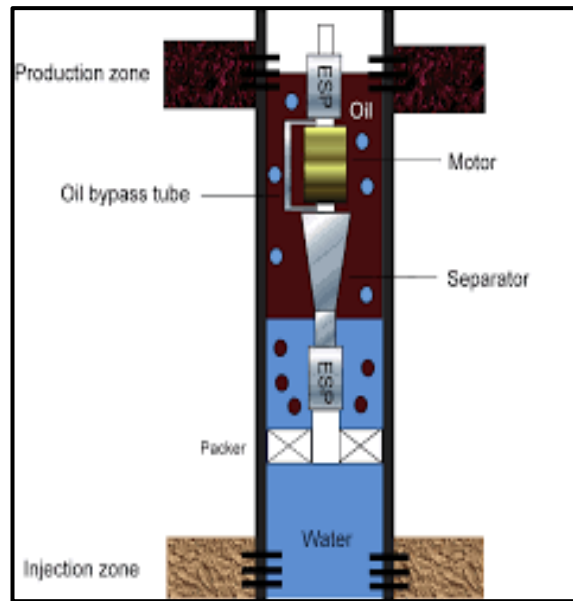


Figure III-9: DOWS with hydro cyclone separator [36].

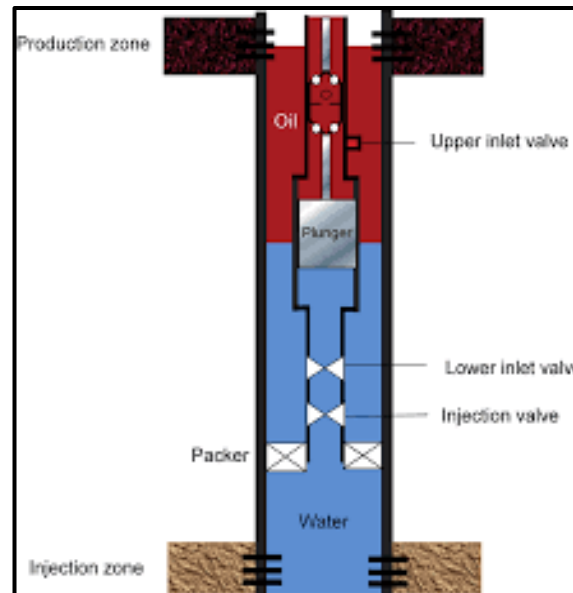
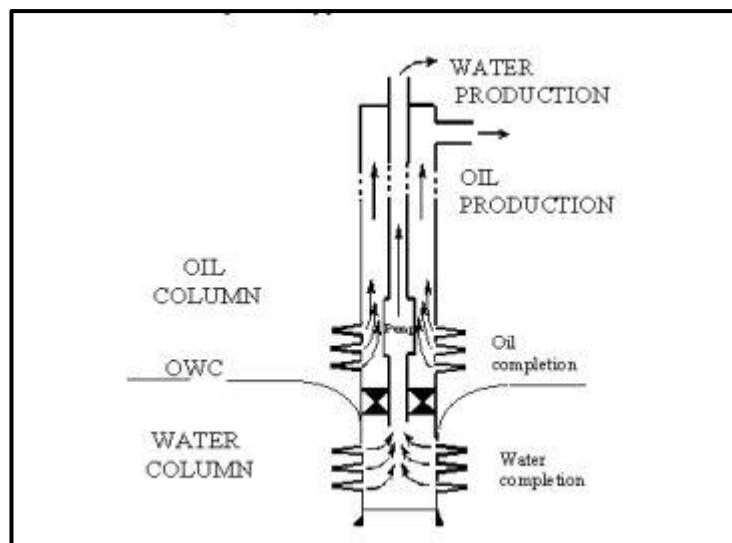


Figure III-10: DOWS with gravity separator [36].

#### III.5.1.4 Downhole water sink technology

Widmyer introduced and patented a novel coning control idea to the petroleum industry known as the downhole water sink (DWS) technology. In his patent, he used two separated completions in one well to control water coning: one produced oil from the oil zone and the other drained water in the aquifer. Thus, the water coning could be controlled by the two opposite pressure drawdowns. The interest of the oil industry was drawn to the DWS technology after Wojtanowicz and Xu improved the technology to a more workable and successful method when they simulated a dual completion using a “tailpipe water sink” as shown in figure III-11. First, an oil well is drilled through the oil bearing zone to the underlying

aquifer. Then, the well is dually completed both in the oil and water zones. A packer separates the oil and water perforations. During production, oil flows into the upper completion being produced up the annulus between the tubing and the casing, while water is drained through the lowermost completion through perforations in the casing and then lifted up through the open tubing below the initial OWC. As a result, the produced oil is water free and the drained water is oil free. Until now, DWS completion has been field tested in numerous reservoirs all over the world with good results. The drawback of this technology is that, it brings large amount of water to the surface which requires more water processing facility and adds the production costs [37].



**Figure III-11:** Schematic of Typical DWS Completion [29].

#### III.5.1.5 Downhole water loop

Downhole water loop (DWL) technology was developed based on downhole water sink (DWS) well/completion to cushion the set back (i.e., handling of a huge volume of water at the surface), experienced with the DWS technology. It involves a triple-completed well: one perforation located in the oil zone and the other two located in the water zone. These three completions are separated by two packers unlike the DWS completion with a single packer. The top most completion at the oil zone is used for oil production while the second completion - water drainage interval (WDI), is used to produce water simultaneously near the oil-water contact to stabilize the interface. The produced water at the WDI is re-injected into the same aquifer through the lowest completion water re-injection interval (WRI) using a submersible pump. A typical configuration of a downhole water loop (DWL) is shown in figure III-12. However, the efficiency of DWL strongly depends upon the vertical distance between the two water looping completions: water drainage and water re-injection intervals. Thus, the

dependence of the DWL technology on water looping completions interval limits its application in reservoir with small size water zone (aquifer) [29].

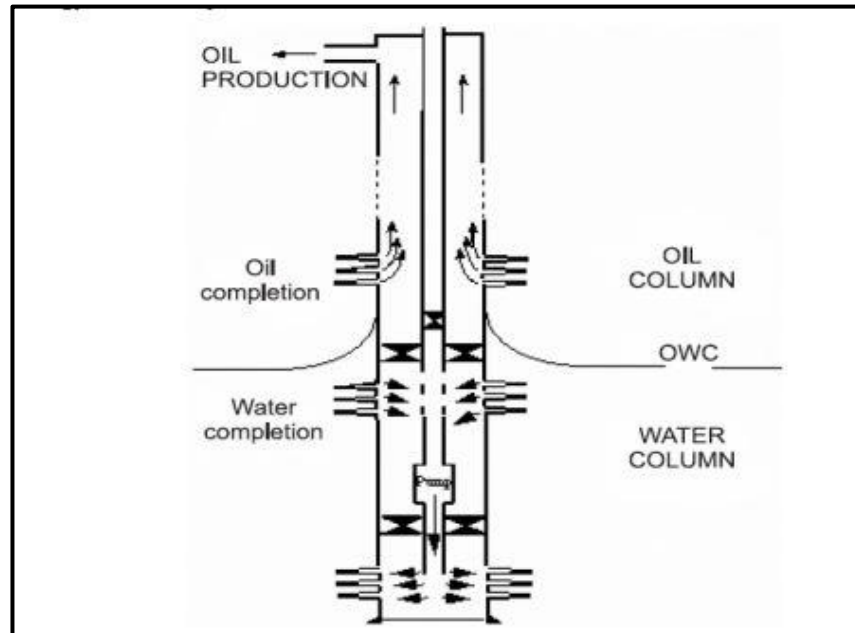


**Figure III-12:** Schematic of Typical DWL Completion [29].

### III.5.1.6 Application of horizontal well technology

Several researchers have recommended horizontal well technology as a solution for the development of reservoirs with water coning problems. While vertical wells act like point source concentrating all the pressure drawdown around the bottom of the wellbore, horizontal wells act more like a line sink and so distribute the pressure drawdown over the entire length of the wellbore. The result is reduced pressure drawdown around the wellbore. Peng and Yeh have shown that the use of horizontal wells is a proven technology for reducing coning problems and improving recovery in reservoirs underlain by water. Various methods have recently been recommended by researchers to improve the productivity of horizontal wells with regard to combating water coning problems. Such as horizontal well completion with a stinger, variation of perforation density, and application of radial drilling technology [37].

### III.5.1.7 Total penetration method

This method typically involves the extension of perforation interval to cross the entire pay zone i.e., oil zone, and into the bottom water zone to maintain the radial flow of fluids. This technique aims to avoid the development of cone and resultant oil bypass. This will result in water production immediately as oil production starts. So, water handling facilities are put in place to accommodate the excessive produced water at the surface. This technology significantly delays the breakthrough time and reduces water cuts. However, over time as production continues the tendency for cone development is unavoidable [29].

### III.5.2 Chemical methods

Near the wellbore or far from the wellbore in the reservoir, the shut-off operations are performed by several chemical treatments. These treatments achieve better performance in the reservoir as well as blocking the undesired water production zones. Chemical treatment aims to block the open features and high permeability channels to force water to go toward the more resistant path to sweep oil from the matrix rock. This will ultimately enhance the overall economic returns [34].

The results of chemical solutions can be achieved in months to years, depending on the nature of the reservoir and the properties of the injected chemicals. There are several chemicals used in treating the water shut-off operations, which are as follows:

#### III.5.2.1 Polymer flooding

Another common technique for water shutoff operations is the usage of the polymer flooding method to increase the viscosity of the water. This technique is applied to increase the viscosity of the drive fluid (water) which helps in mobilizing and displacing the oil in the reservoir matrix rock. This technique is usually applied in the reservoir far from the production wells through water injection wells to achieve better sweeping efficiency in the reservoir. That eventually leads to preventing excessive water production. The usage of polymer flooding is very common among the oil operators and it can be prepared by dissolving the polymers in the injected water and injecting it through injection wells. Polymers used in this technique are usually two types: biopolymers and synthetic polymers. Biopolymers' advantages over the synthetics are that they are not affected by the salinity of the water and they are insensitive to mechanical degradations. However, they are more expensive than synthetic polymers [34].

#### III.5.2.2 Gel injection

Gel injection is one of the most well-known chemical treatments for water shutoff operations and is used to reduce the water oil ratio (WOR) and increase the conformance of the pattern. This process is done by the ability of the gel to reduce the permeability and block the open features, fractures, and high permeability water zones. The injected gel is mainly made of water, small volumes of polymers, and crosslinking chemical agents. Gel treatments can entirely seal off layers; therefore, they are considered aggressive and risky conformance control operations. In contrast, polymer gel injection is considered relatively cheaper than other improved oil recovery operations. Gel injection operations are classified into three main stages: modeling, designing, and executing, and are used accordingly [34].

# *Chapter IV*

*Optimizing oil production in  
the Amassak field: diagnosing  
and mitigating water coning*





The region currently has 18 operating perimeters (figure IV-3).

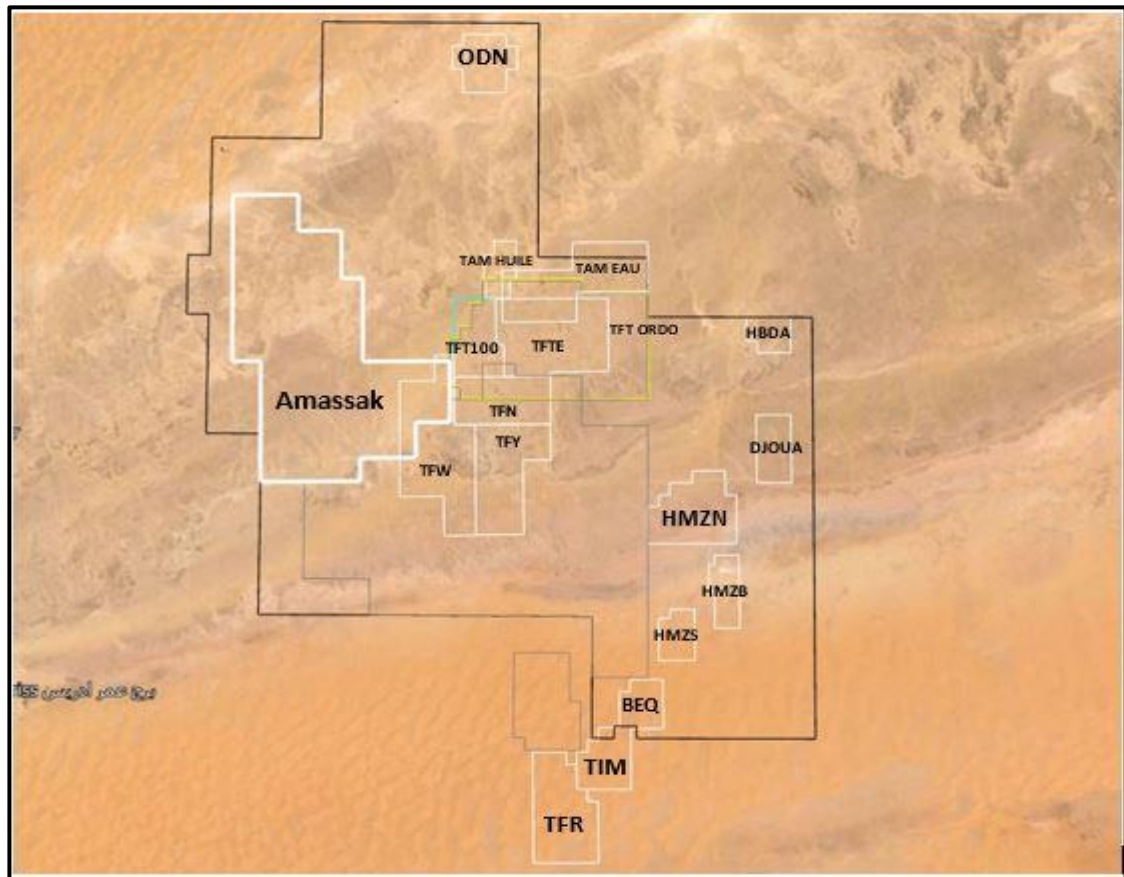


**Figure IV-3:** Geological location of the 18 perimeters in the TFT area [38].

#### IV.1.1 Amassak field background

The Amassak field is one of the main oil-producing fields of the TFT area, discovered in 1970 and started production in 1974, located in the Illizi basin in the eastern part of the Algerian Sahara, 30.5km west of the TFT field. It is currently developed by 94 wells for its oil ring located on the eastern flank of the structure, limited to the west by a major fault. Oil and gas have been identified in unit IV-3 of the Ordovician which is the main reservoir in this area with a pressure equal to 145 bars and an operating temperature of about 85°C.

##### IV.1.1.1 The Ordovician reservoir

The Ordovician reservoir appears as a monocline sloping towards the north-east and intersected by several submeridian accidents; these accidents act as limits to the oil accumulation compartments. The wells that our study is based on are producing from the two Ordovician units IV-3 and IV-2.

**Unit IV:** The Unit IV formation has an average thickness of 100 to 300 meters. It is composed of glacial sandstone and clay. This formation unconformably overlies the Unit III-3.

Unit IV comprises two main sub-units:



**Unit IV-3:** Characterized by the predominance of generally medium coarse and clean sandstones and is observed locally by a passage between clean sandstones and clayey sandstones and even clayey-sandstone facies. (Predominantly sandstone)

**Unit IV-2:** This is a series of infill deposits that filled the paleotopographies shaped by the advance of glaciers. It is composed of varied sedimentary deposits. (Predominantly clay-sandstone) [38].

#### **IV.1.2 HBDA field background**

The Hassi Belhouda (HBDA) oil field is a significant oil reserve located in the east of the TFT region in In Amenas, Illizi, Algeria. This field is known for its substantial recoverable initial reserve of 3.73 MMm<sup>3</sup>. As of March 10th, 2024, it has accumulated a production of 0.56128 MMm<sup>3</sup>. The oil reservoir is identified as Devonian Unit CIII-1, B, A at M1-X with a pressure ranging from 160-190 bars and an operating temperature of about 80°C.

The drilling at the HBDA1 well was conducted in November 19th, 2011. The development of the HBDA field includes several drilling operations and equipment installations. In 2019, the HBDA6, HDBA7, HDBA8, HDBA9, and HDBA10 wells were drilled. The forecast for 2024 includes the drilling of the HBDA11 well.

The field also saw the implementation of fracture operations in 2019 at the HDBA2 and HBDA8 wells. Short radius drilling was carried out in 2022 at the HBDA6 well, and similar operations are planned for 2024 at the HBDA10 well.

The field has been equipped with ESP at the HBDAA2, HBDA5, HBDA6, HBDA7, and HBDA wells in the years 2021, 2022, and 2023. This comprehensive development plan aims to maximize the extraction of the oil reserves in the HBDA field [38].



Figure IV-4: Well locations in HBDA field [38].

#### IV.1.2.1 The Devonian reservoir

The Devonian series is characterized by the absence of middle Devonian terms.

##### 1. Upper Devonian:

- a. **Strunian:** It consists of black-gray, silty, micaceous clay, with intermittent metric levels of medium to coarse brown sandstone, silty-clayey, and pyritic.
- b. **Clayey Series:** This interval is composed of dark gray to black, silty clay, finely micaceous, and soft white silt.

##### 2. Lower Devonian (F6):

- a. **Unit C3-I:** Characterized by alternating layers of clay and sandstone.
- b. **Unit C2-II:** Interbedded with metric levels of white, fine to very fine, friable sandstone, poorly cemented, interspersed with dark gray, silty clay, finely micaceous, and soft white silt.

- c. **Unit C1-III (Thickness: 15m):** Comprises layers of well-sorted, medium to coarse white sandstone, siliceous, rich in quartz grains, separated by layers of dark gray, silty clay, finely micaceous, and indurated soft white silt [38].

**IV.1.3 DATA collection**

Obtaining data from the Reservoir is the first step towards completing this thesis. Data type (permeability thickness, stock tank oil, water density, pay-zone thickness, and horizontal and vertical permeability) were used to conclude this analysis with precision.

**IV.1.3.1 Amassak field**

**a) Reservoir fluid properties**

**Table IV-1:** Reservoir fluid properties in Amassak field.

Fluid property	Symbol (Units)	Value
Initial pressure of the reservoir	P <sub>i</sub> (bars)	202
Temperature of the reservoir	T (°C)	85
Saturation pressure	P <sub>b</sub> (bars)	202
FVF initial	B <sub>oi</sub> (RB/STB)	1.472
Solution GOR	R <sub>Si</sub> (SCF/STB)	161.5
Oil density	d <sub>o</sub> (g/cc)	0.819
Oil viscosity	μ <sub>o</sub> (cp)	0.365

**b) Reservoir rock properties**

**Table IV-2:** Reservoir rock properties in Amassak field.

Rock property	Symbol (Units)	Value
Average porosity	Ø (%)	9
Permeability	K (mD)	60
Water Saturation	Sw (%)	21
Reservoir thickness (IV-3 Unit)	H (ft)	52.493

**IV.1.3.2 HBDA field**

**a) Reservoir fluid properties**

**Table IV-3:** Reservoir fluid properties in HBDA field.

Fluid property	Symbol (Units)	Value
Initial pressure of the reservoir	Pi (bars)	200
Temperature of the reservoir	T (°C)	80
Saturation pressure	Pb (bars)	200
FVF initial	Boi (RB/STB)	1.47
Solution GOR	RSi (SCF/STB)	161.5
Oil density	do (g/cc)	0.819
Oil viscosity	$\mu_o$ (cp)	0.365

**b) Reservoir rock properties****Table IV-4:** Reservoir rock properties in HBDA field.

Rock property	Symbol (Units)	Value
Average porosity	$\emptyset$ (%)	14
Permeability	K (mD)	60
Water Saturation	Sw (%)	35
Reservoir thickness (C1-III Unit)	H (ft)	49

**IV.2 The impact of water cut on the oil production rate****IV.2.1 History analysis of water cut and oil production rate**

The data collected from wells AMA 73 and AMA 75 aim to explore the relationship between water cut and production flow rate, analyzing their impact on each other. The histogram below illustrates this comparison, shedding light on how variations in water cut influence production flow rates in both wells.

The well AMA 73:

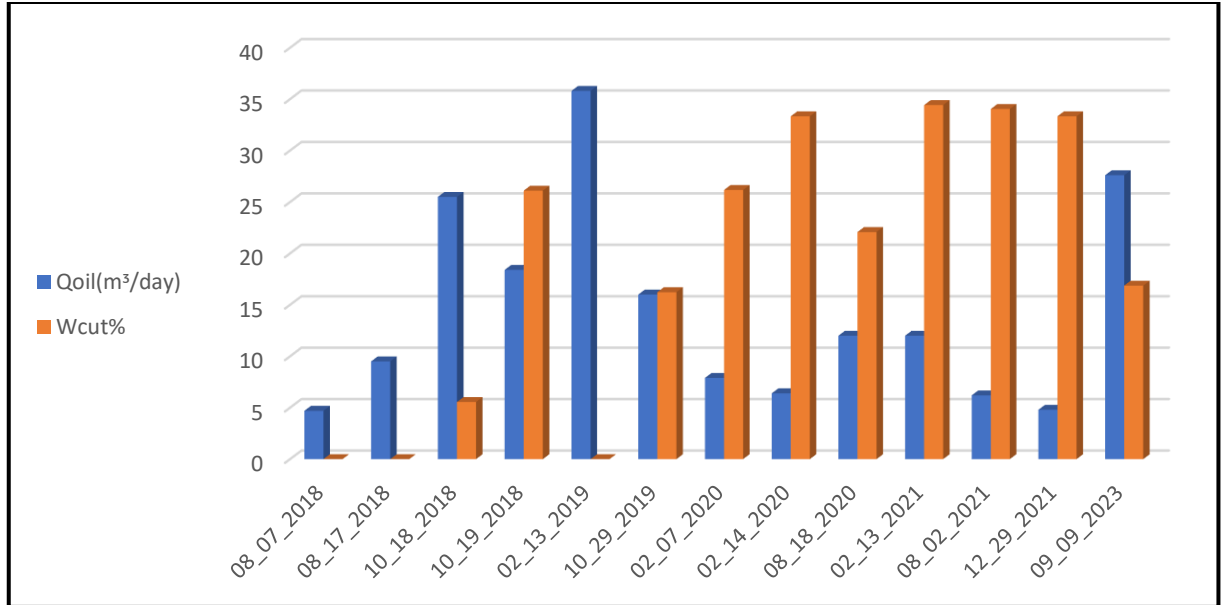


**Figure IV-5:** Impact of water cut on production flow rate in AMA 73.

The well AMA 75:

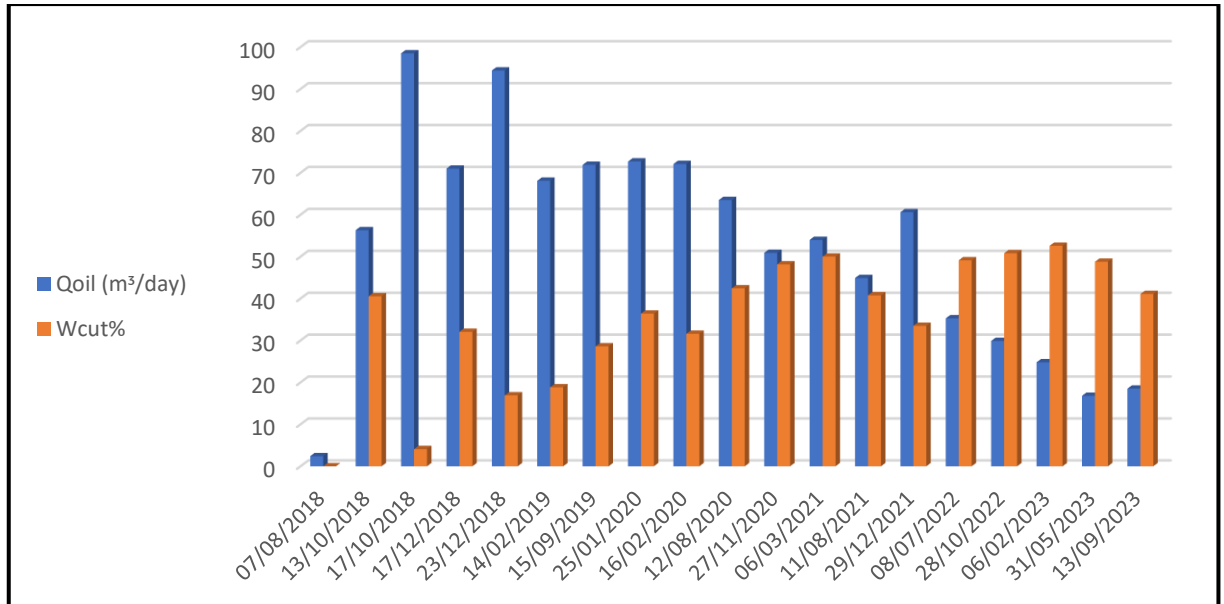


**Figure IV-6:** Impact of water cut on production flow rate in AMA 75.

Our analysis reveals a notable impact of water cut on the oil production rate of the wells. As the water cut increases, there is a discernible decrease in the production rate of the oil observed in both wells AMA 73 and AMA 75.

## IV.2.2 Simulation Analysis using PROSPER

Using PROSPER simulator, we set up a simulation model for the well AMA 73 and conducted a sensitivity analysis specifically focused on the water cut parameter to understand water cut impact on oil production.

### IV.2.2.1 Description of PROSOER simulator

PROSPER is simulator software that is a part of Integrated Production Modelling (IPM). PROSPER is widely used in the oil and gas industry to design and optimize well performance as shown in figure IV-7, from single to multilateral wells. The software is capable of modelling and optimizing most types of well completion and artificial lift methods. Nodal analysis is used to perform sensitivity analysis for different operating conditions, allowing for accurate calculations and better results. It generates separate models for each component of the well system, which can be verified through performance matching to ensure accuracy [39].

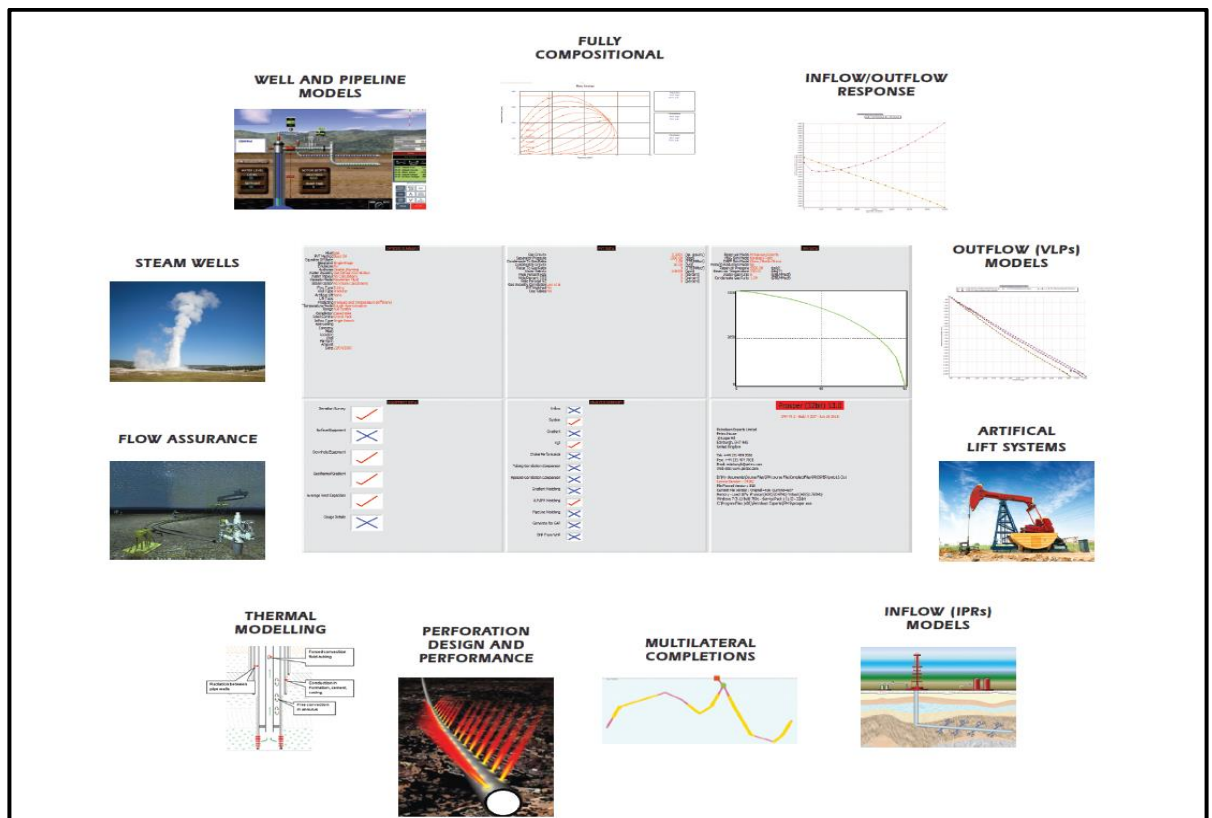


Figure IV-7: PROSPER software interface and utilizations [39].

### IV.2.2.2 Simulation steps

The simulation study passes through some essential steps:

- Data Collection: We began by collecting comprehensive data on fluid properties, as well as PVT parameters, from well tests and laboratory analyses conducted in the Amassak oil field, detailed data on gas lift operation for its influence on fluid behaviour

and production dynamics, such as gas injection rates, in addition to Well characteristics and production history were collected for accurate modelling.

- Model Setup: A well model for well AMA 73 was created in PROSPER, with the collected data such as reservoir parameters, fluid properties, and well configuration. Involved in matching the PVT parameters obtained from well tests and laboratory analyses to initialize the simulation model.
- Scenario Analysis: Various scenarios were simulated, focusing on different levels of water cut to observe their effects on oil production rates.

### IV.2.2.3 Results

After validation of the model, we simulated with different water cut settings (0,30 and 60 percent) and then observed how it affected the oil production rates at the well AMA 73. Our findings are summarized in the chart below (Figure IV-8).

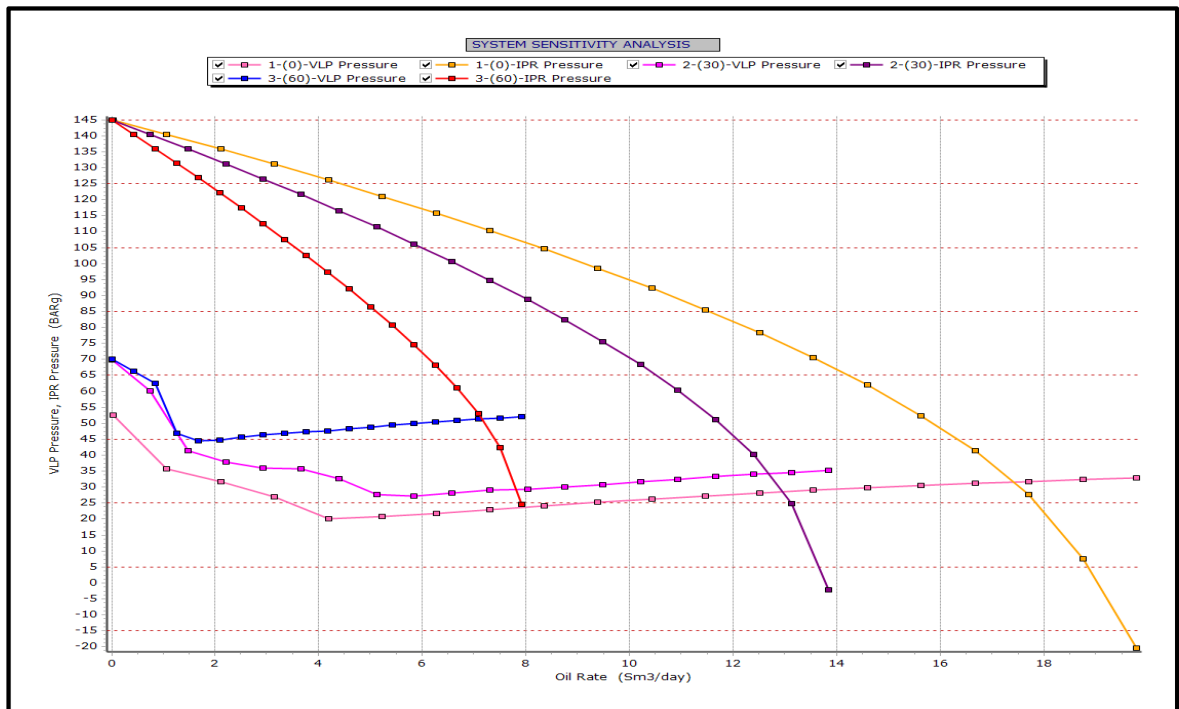


Figure IV-8: Water cut sensitivity analyses.

This simulation allowed us to observe how different levels of water cut influence the oil output. We can notice that with high water cut levels, the oil production rate decreases. At first, when the water cut is 0%, the oil production rate is 17.71 Sm<sup>3</sup>/day. However, as the water cut increases to 30% and 60%, the oil production rates decline to 12.4 and 7.5 Sm<sup>3</sup>/day, respectively.



IV.2.2.4 Discussion of results

After analyzing both real and simulation results, the rate of the produced fluid (oil/water) decreases because the column is getting heavier due to the water specific gravity. Then the produced water starts increasing because of its high mobility comparing to oil's.

IV.3 Case study 1: Problem diagnosis

IV.3.1 Chan plot

In our pursuit to identify the factors influencing water cut in our wells, we turn to Chan plots as a diagnostic tool.

The well AMA 73:

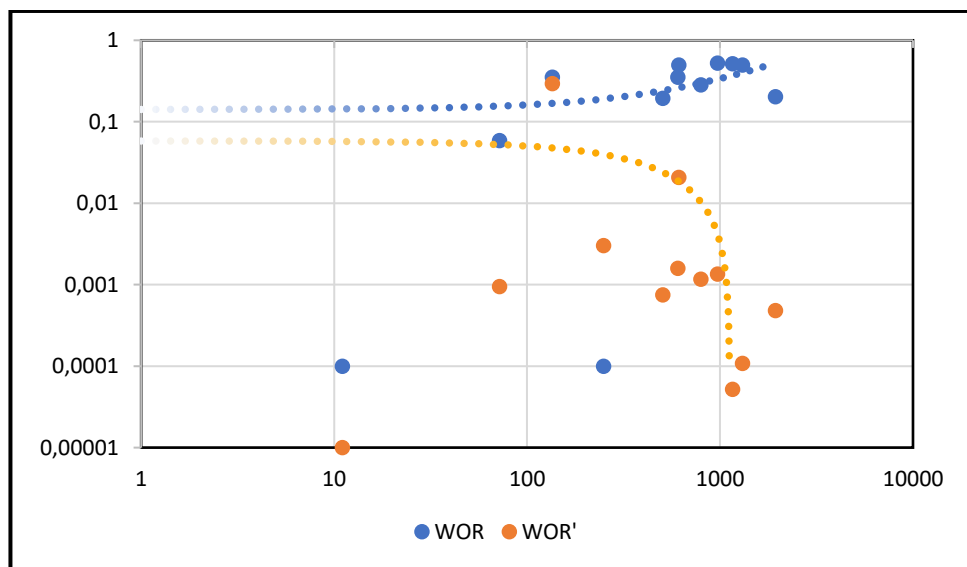


Figure IV-9: Well AMA 73 Chan plot.

The well AMA 75:

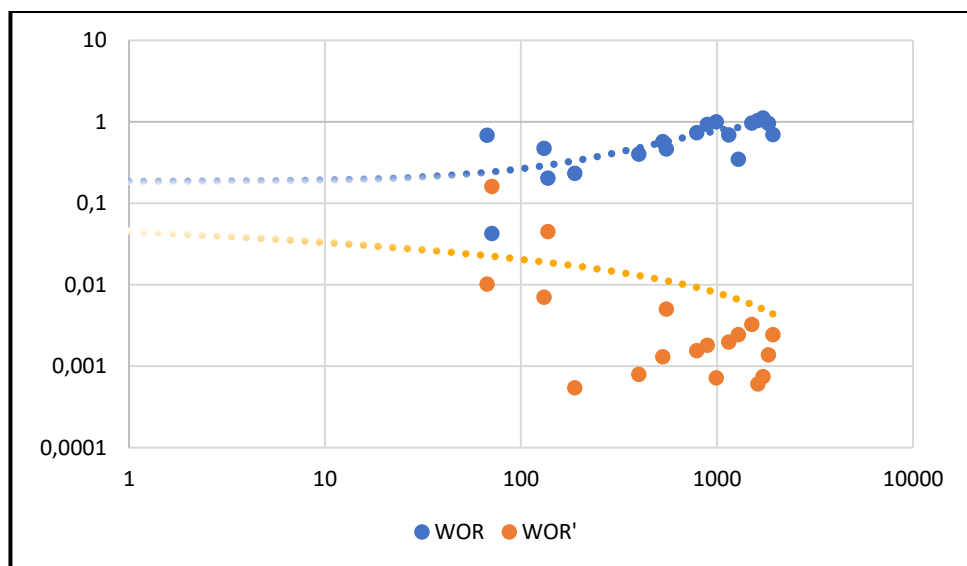


Figure IV-10: Well AMA 75 Chan plot.



Upon analyzing the Chan plots for the wells AMA 73 and AMA 75 the diagnostic plots between WOR (Water Oil Ratio) and WOR derivatives versus time were identified.

### IV.3.2 Determination of critical production rate

As mentioned in chapter III, operating the well at a production rate below the critical threshold can effectively postpone the onset of water coning. Meyer-Garder and Chaney et al equations (Eq III-1, Eq III-2) have been used to determine the critical production rate in this study. The results achieved as follows:

The well AMA 73:

**Table IV-5:** Critical Oil Rate correlation results in well AMA 73.

Correlation	Critical oil rate $Q_{oc}$	Unit
Meyer-Garder	4.342871	STB/Day
Cheney et al	9.274302	STB/Day

Table IV-5 shows that the correlations give values of critical rate with low values, the critical oil rates vary from 4.342871 STB/day to 9.274302 STB/day, where the measured oil rate was 59.75 STB/Day.

The well AMA 75:

**Table IV-6:** Critical Oil Rate Correlation Results, Well AMA 75.

Correlation	Critical oil rate $Q_{oc}$	Unit
Meyer-Garder	7.716296	STB/Day
Cheney et al	16.71831	STB/Day

Table IV-6 shows that the correlations give values of critical rate with low values, the critical oil rates vary from 7.716296 STB/day to 16.71831 STB/day, where the measured oil rate was 379 STB/Day.

### IV.3.3 Water Breakthrough Time

#### a) Breakthrough time calculations

The Sobocinski-Cornelius method (Eq III-12) is contrasted with the Bournazel-Jeanson method (Eq III-14), in which associations formed both through experimentation and using dimensional parameters. The outcome varies because of the difference between their functional variables, mostly because of the dimensional breakthrough period. The findings of the

distinction between the Sobocinski-Cornelius approach and the Bournazel-Jeanson approach are shown in (Table IV-7).

**Table IV-7:** Water Breakthrough time for AMA 73 and AMA 75.

Correlation	Breakthrough Time (days)	
	AMA 73	AMA 75
Sobocinski-Cornelius	118	33
Bournazel Jeanson	54	17

**b) Water Breakthrough Time prediction with different flow rates**

Based on the Sobocinski-Cornelius method (Eq III-12), a simulation study was conducted to predict the water breakthrough time over different flow rates. The results are shown in figure IV-11 and figure IV-12.

The well AMA 73:

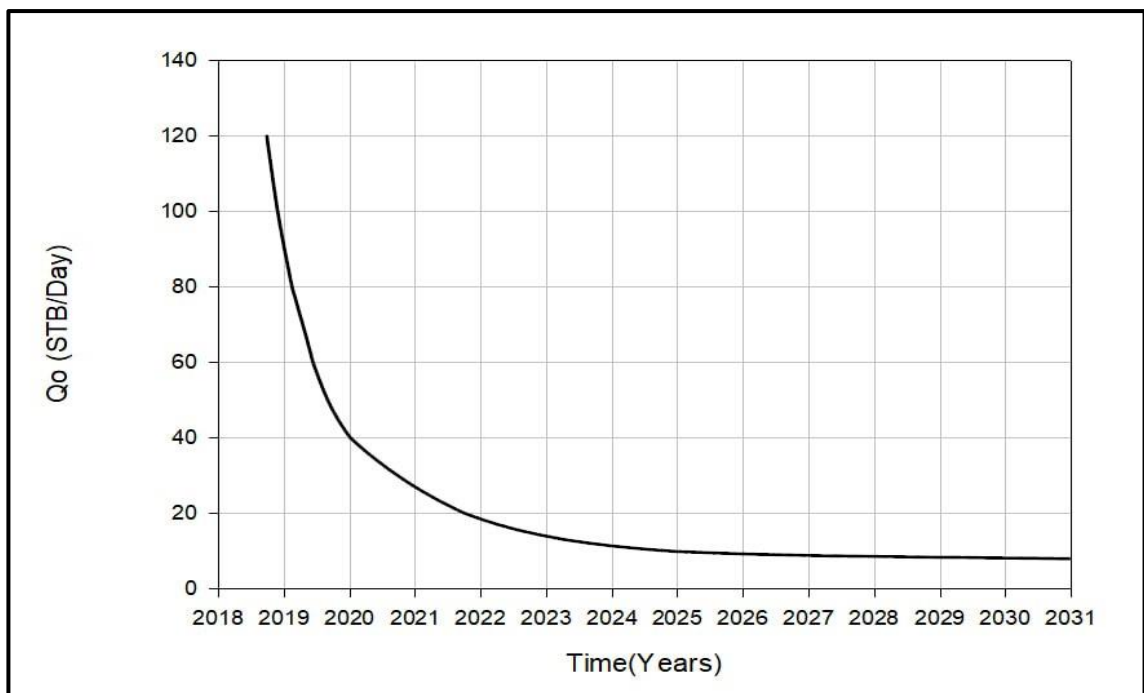


**Figure IV-11:** predicting water breakthrough time with difference flow rates for AMA 73.

The Well AMA75:

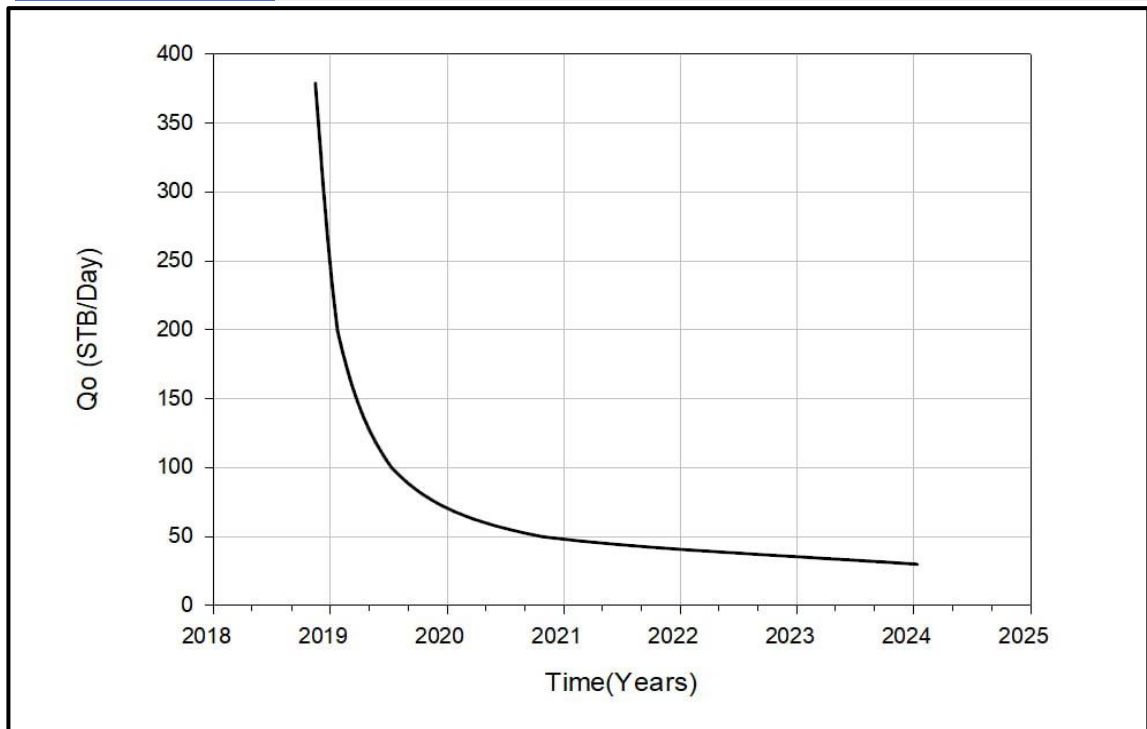


**Figure IV-12:** predicting water breakthrough time with difference flow rates for AMA 75.

#### IV.3.4 Discussion of results

- The plots show that the WOR derivatives have negative slope values, which is consistent with the pattern observed in the water coning Chan plot. This similarity suggests that wells AMA 73 and AMA 75 are experiencing water coning. (After comparing figure IV-9 and figure IV-10 with figure III-3)
- While reducing the production rate can help delay water coning, the critical production rates calculated to prevent this phenomenon are often considered uneconomic. (See table IV-5 and table IV-6).
- Based on the analysis of breakthrough time for AMA 73 and AMA 75 using old data, the simulated breakthrough times exhibit an approximate resemblance to the real breakthrough times. For AMA 73, the real and simulated breakthrough times are approximately between 54 and 118 days. Similarly for AMA 75, the real and simulated breakthrough times are approximately between 18 and 33 days (Table IV-7).
- The plots generated from the simulations, showed a clear trend: as the flow rates increased, the breakthrough time occurred earlier, which confirms that higher production rates over critical rate accelerate the water breakthrough. (Figure IV-11 and Figure IV-12).

**IV.4 Case study 02: Water coning risks in artificial lift operations**

Oil wells naturally experience a decline in pressure as oil is extracted. Artificial lift methods are employed to maintain sufficient pressure and continue production. However, while artificial lift is necessary for oil production, some methods can inadvertently contribute to water coning. In this exploration, we will compare the influence of the electrical submersible pumps (ESPs) and Gas lift (GL) on water coning.

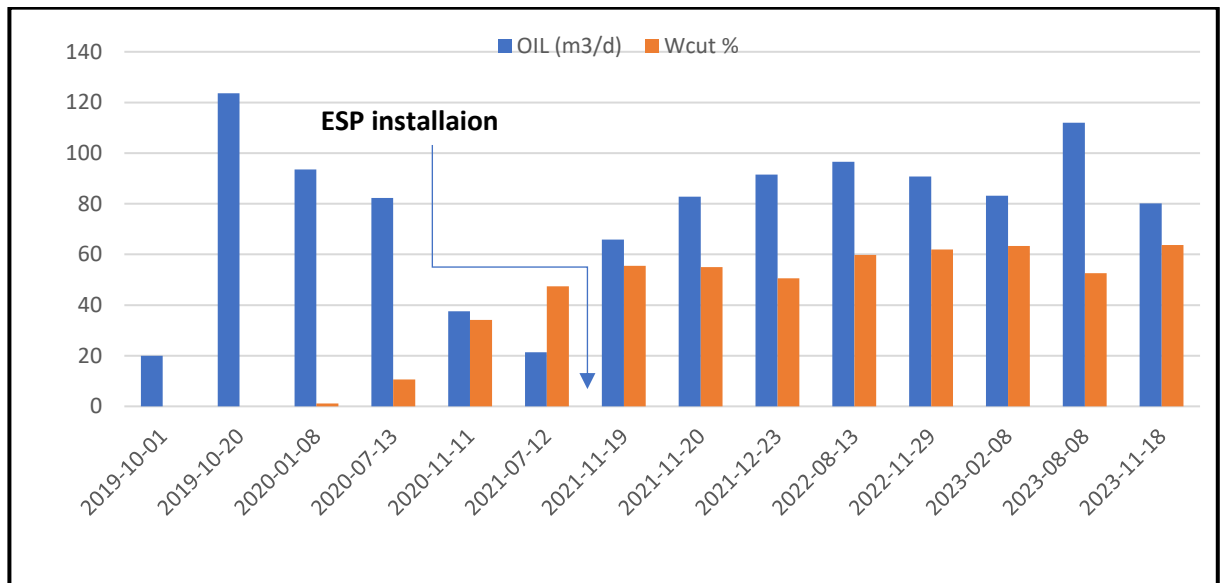


**Figure IV-13:** Oil production rate and water cut performance before and after ESP installation in the well HBDA1.

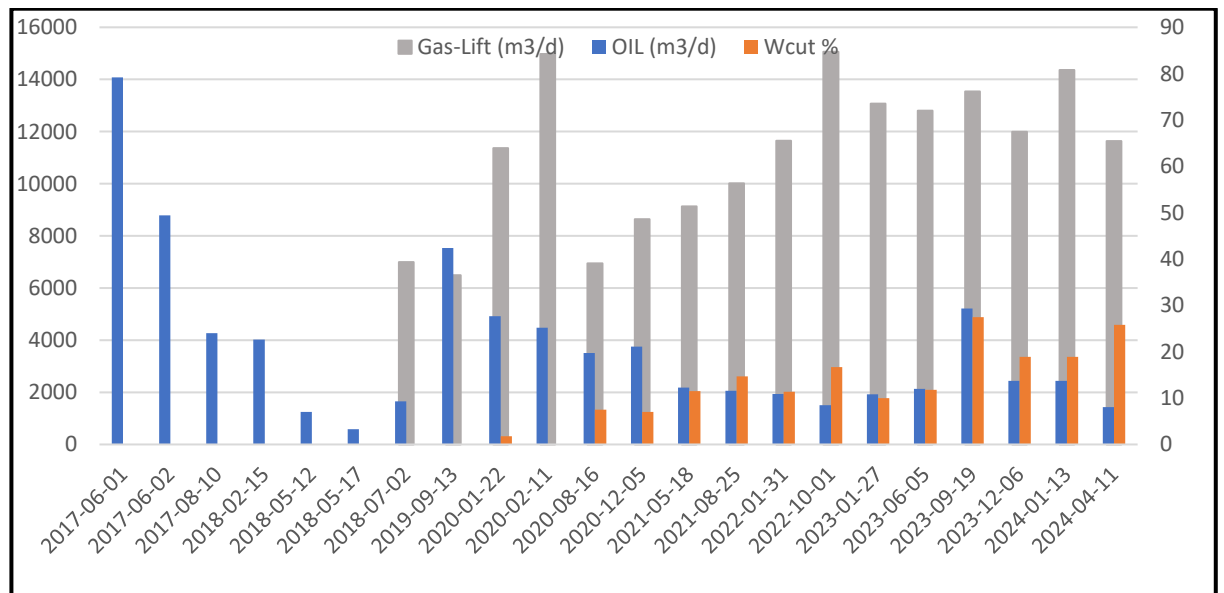


**Figure IV-14:** Impact of GL on the performance of oil production rate and water cut in the well AMA69.

Figure IV-13 shows the histogram of  $Q_{oil}$  and water cut versus time for well HBDA1 before and after installing the electrical submersible pump. The result shows that the  $Q_o$  has

reduced significantly to 21 m<sup>3</sup>/d from 120 m<sup>3</sup>/d before using the ESP, while after implementing the ESP, the Q<sub>o</sub> has increased significantly to 112 m<sup>3</sup>/d. Additionally, water cut before and after ESP installation is shown in figure IV-13. The results indicated that the water cut percentage has increased after implementing ESP and reached 63.62%.

Figure IV-14 represents the oil flow rates and water cut percentage over time for the well AMA69 before and after using gas lift. The results show that the Q<sub>o</sub> was reduced from 79.2 m<sup>3</sup>/d to 3.3 m<sup>3</sup>/d, while after injection gas, it increased again and reached 42.2%. We can notice that the water cut percentage increased after an over injection of gas and went from 0 to 27.48%. Where gas injection leads to increased oil flow rates, it causes water cut augmentation over time.

#### IV.4.1 Discussion of results

- **Electrical Submersible Pumps (ESP):** These pumps are placed downhole and directly lift fluids to the surface. They are highly efficient but can create a strong pressure drawdown around the wellbore. This pressure reduction can pull water from the surrounding formation, potentially accelerating water coning, particularly in thin oil zones.
- **Gas Lift:** This method injects gas down the wellbore to lighten the fluid column and enhance production. While gas lift generally has a lower impact on pressure drawdown than ESPs, uneven gas distribution is a potential concern. If the gas isn't distributed uniformly across the producing zone, it can create channels where water can flow more readily, leading to water coning. Additionally, high gas injection rates can disrupt the water-oil interface within the reservoir, promoting water influx.
- **Higher Production, Higher Risk:** While ESP offer the advantage of higher production rates, they also carry a higher potential to exacerbate water coning due to the strong pressure drawdown it creates.
- **Lower Production, Lower Risk:** Gas lift generally has a lower pressure drawdown impact and can be a better choice for reservoirs prone to water coning. However, it may result in lower production rates compared to ESP.

#### IV.5 Case study 3: Short radius as a mitigation technique

In this study, we delve into the application of short radius in the well HBDA6 as a strategic solution to address the challenging issue of water coning in oil wells.

We seek to investigate the efficacy of short radius in controlling water coning,

improving oil recovery rates, and enhancing the overall operational efficiency of oil wells facing water production issues.

**HBDA 6 Well overview:**

The well HBDA6 was drilled in November 2019 and encountered an enough high-pressure reservoir, allowing it to flow naturally to the surface without artificial lift (eruptive well).

In July 2022, a **short radius** was drilled from the original well (Figure IV-15).

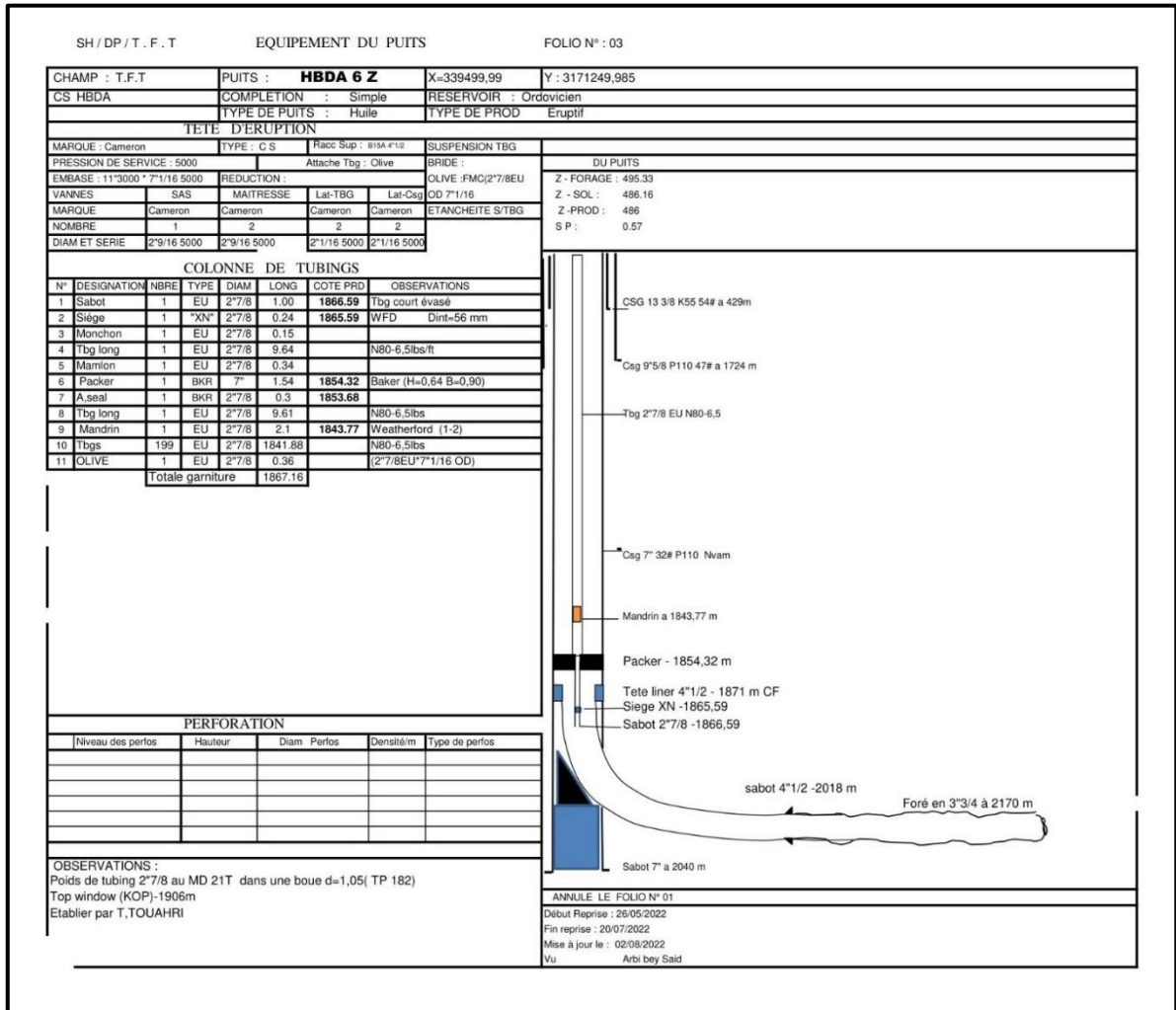


**Figure IV-15: Well HBDA6 technical sheet [38].**

The well's production performance before and after the short radius sidetrack operation is shown in Figure IV-16.

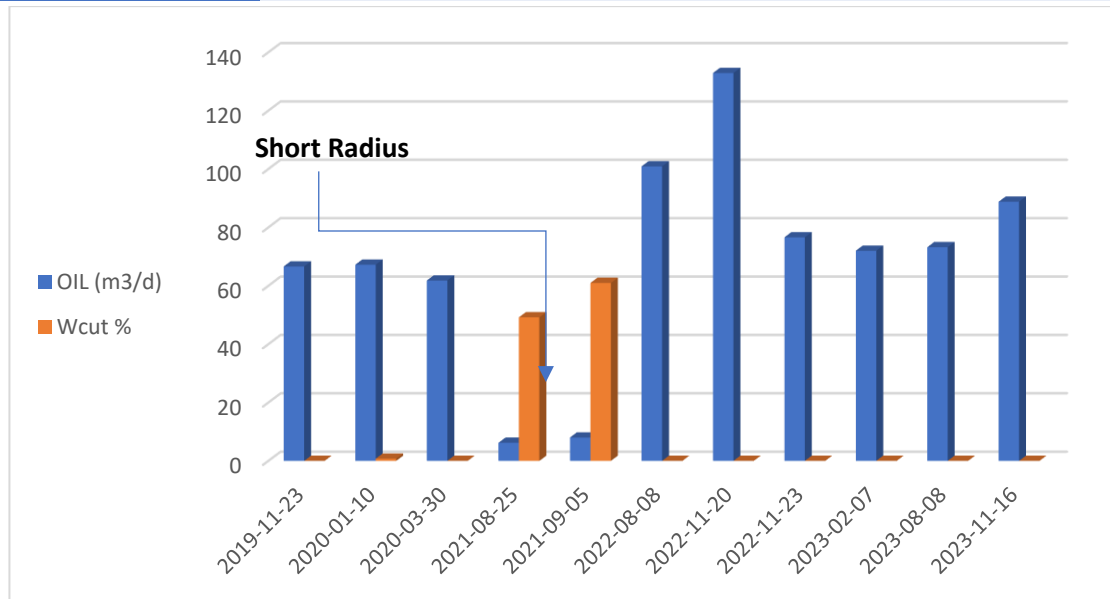


**Figure IV-16:** Oil rate and water cut performance in HBDA6.

Before the short radius implementation, the well exhibited a high water cut reached up to 61%, with water production making up a significant portion of the total fluids produced. However, after the short radius was drilled, the water cut was completely eliminated, with a remarkable increase of oil rates (up to 133 m<sup>3</sup>/day).

#### IV.5.1 Discussions of results

In our case, the high water cut caused by water coning due to the well's high production rate and the proximity of the production zone to the water-oil contact (because of the thinness of our reservoir). The short radius was successful in mitigating this issue by precisely placing the new wellbore to avoid the water-bearing zones and reduce water influx, while still accessing the oil.

In such conditions, short radius as part of optimizing well placement is a key strategy to manage water coning problems.

*Conclusion and  
Recommendations*



## Conclusion

In our thesis, we have analyzed the negative impacts of water coning on the performance of the Amassak and Hassi Belhouda oil fields. Fundamental features of reservoir parameters, well performance, water coning phenomena, and different case studies from this oil field have been studied. Our analysis has led us to the following conclusions:

- Water cone formation displaces oil near producing wells, thereby reducing the effective oil production zone. As a result, less oil is produced from the reservoir, reducing the overall oil production rate and increasing the water cut, as the performance study in the wells AMA 75 and AMA 73 shows, where the production rate significantly reduced from (35.45 to 4.8)  $\text{sm}^3/\text{day}$  and (94.4 to 16.8)  $\text{sm}^3/\text{day}$  respectively.
- The Chan Plot is a very useful and accurate diagnostic tool. For the determination of water coning: Two wells were studied from the Amassak oil field and showed a water coning behaviour.
- The results of the critical rate calculation indicate very low values for the wells AMA 73 and AMA 75  $Q_c=9.274302$  STB/Day,  $Q_c=16.71831$  STB/Day respectively, which implies that producing oil from the reservoir at rates below this critical threshold is not possible due to economics constraints.
- Due to the reservoir properties and high production rates, the breakthrough time becomes significantly short (33 days for AMA73 and 18 days for AMA75) and at lower production rates, we achieve a favorable breakthrough time.
- While artificial lift can effectively lift fluids from the reservoir to the surface, inappropriate selection or improper implementation of artificial lift methods can indeed cause water coning.
- Gas lift, can typically delay water coning compared to ESP. However, when high injection rates are employed with gas lift, it can inadvertently contribute to faster water coning. In our case, the water cut of well AMA 69 reaches 20% after a high gas lift injection rate of 14976  $\text{Sm}^3/\text{day}$ .
- Short-radius can significantly mitigate water coning effects, reducing water cut and improving oil recovery, in the well HBDA 6 water cut was significantly reduced from 60.98% to 0%.

### **Recommendations**

After a thorough analysis of water coning and its impacts on the performance of the Amassak and Hassi Belhouda oil fields, we recommend the following strategies to mitigate water coning and optimize oil production:

- Maintain lower production rates as close to the critical rate as possible, ensuring that production remains profitable and increases the life cycle of the wells.
- A careful consideration of artificial lift design and operation is essential to avoid the risk of accelerated water coning and maintain optimal reservoir performance.
- Implement horizontal or short-radius wells as a mitigation and prevention technique to provide a larger contact area with the oil zone and delay water breakthrough time.
- Using advanced monitoring technologies to track wells performance and water cut may allow for predicting water coning and developing timely production strategies and interventions.
- An advanced reservoir simulation study can be integrated into our thesis to predict water coning behaviour and plan appropriate mitigation strategies.

# *References*

*References*

- [1] S. Osisanya, R. Recham and M. Touami, "Effects of Water Coning on the Performance of vertical and horizontal wells A Reservoir simulation study of Hassi R'Mel Field, Algeria," p. 13, 2000.
- [2] F. Mekunye and P. O. Ogbeide, "Application of Chan Plot in Water Control Diagnostics for Field Optimization: Water/Gas Coning and Cusping," *NIPES Journal of Science and Technology Research*, pp. 1-7, 2021.
- [3] I. Igwe, F. O. Wopara, A. I. Echeonwu and P. Anucha., "EVALUATION OF WATER PRODUCTION EFFECT ON RESERVOIR PERFORMANCE USING DIAGNOSTIC PLOTS," *International Research Journal of Modernization in Engineering Technology and Science* . , vol. 06, no. 03, pp. 7-9, 2024.
- [4] T. Ahmed, reservoir engineering handbook second edition, Boston • London • Auckland • Johannesburg • Melbourne • New Delhi: Gulf Professional Publishing, 2001.
- [5] T. A.-A. Omar, Fundamentals of Reservoir rock properties, Switzerland AG: Springer Nature, 2020.
- [6] N. Alyafei, Fundamentals of reservoir rock properties 2 nd edition, Doha Qatar: Hamad Bin Khalifa University Press, 2021.
- [7] M. Amirpour, S. R. Shadizadeh, H. Esfandyari and S. Ahmadi, "Experimental Investigation of Wettability Alteration on Residual Oil Saturation Using Capillary Pressure Measurement," *Pertroleum*, pp. 8-12, 2015.
- [8] S. Thomas, "Enhanced Oil Recovery – An Overview," *Oil & Gas Science and Technology* , vol. 63, no. 1, pp. 9-19, 2008.
- [9] A. Y. Dandekar, Petroleum Reservoir Rock and Fluid Properties, CRC Press, March 20, 2013.
- [10] L. Dake, Fundamentals of Reservoir Engineering, Elsevier, , 1983.

- [11] R. v. Flatern, "https://www.slb.com," 01 01 2015. [Online]. Available: <https://www.slb.com/resource-library/oilfield-review/defining-series/defining-esp..> [Accessed 15 5 2024].
- [12] T. Ahmed and P. D.Mckinney, *Advanced Reservoir Engineering*, ELSEVIER, 2005.
- [13] G. R. Elliott, "Behavior and Control of Natural Water-drive Reservoirs," *SPE international*, vol. 165, no. 01, p. 01, 1946.
- [14] G. King, "Dutton institut," [Online]. Available: <https://www.e-education.psu.edu/png301/node/508>. [Accessed 21 04 2024].
- [15] S. R. Sills, "AAPG WIKI," [Online]. Available: [https://wiki.aapg.org/Drive\\_mechanisms\\_and\\_recovery](https://wiki.aapg.org/Drive_mechanisms_and_recovery). [Accessed 21 04 2024].
- [16] M. Golan and C. H. Whitson, *Well Performance*, Springer Dordrecht, 31 August 1987.
- [17] g. takacs, *Electrical submersible pumps manual (second edition) design operations and maintenance*, Gulf Professional Publishing , 2018.
- [18] J. V. Vogel, "Inflow Performance Relationships for Solution-Gas Drive Wells," *Journal of Petroleum Technology*, 1968.
- [19] M. Tuzovskiy, "Wiki pngtools," [Online]. Available: <https://wiki.pengtools.com/index.php?title=VLP>. [Accessed 20 05 2024].
- [20] O. C. Wilfred and F. O. Samuel, "COMPARATIVE EVALUATION OF ARTIFICIAL LIFT METHODS," *Academic Research International*, vol. 7, no. 1, pp. 3-5, January 2016.
- [21] O. Sylvester, I. Bibobra and O. Augustina, "Gas Lift Technique a Tool to Production Optimization," *International Journal of Oil, Gas and Coal Engineering* (Volume 3, Issue 3), 11 June 2015.
- [22] C. S. Bakiler, "PETE 332, *Petroleum Production Engineering*", 02.03.2012.


- [23] D. Hadzihafizovic, "Artificial lift methods," *Journal of Petroleum Geology*, pp. 13-32, octobre 2023.
- [24] L. R. Pineda, A. L. Serpa and Jorge L. Biazussi, "Online trained controller for Electrical Submersible Pumps in liquid–gas flow,," *Geoenergy Science and Engineering*, vol. 225, 2023.
- [25] M. A. A. Al-Ali, V.Kornilov and A.Gordonov., "optimize the performance of electrical equipement in gas separation stations (degassing station ds) and electrical submersible pumps of oil equipement for oil rumaila field," *Published in Proceedings of the higher Engineering Environmental Science* , pp. 15-29, 11 April 2019.
- [26] M. Jadid, A. Lyngholm, M. Opsal and A. Vasper., "The pressure's on: Innovations in gas lift," *Research gate* , vol. 8, pp. 44-53, decembre 2006.
- [27] W. Renpu, *Advanced well completion engineering*, Elsevier , 2011.
- [28] "Studocu.com," 2019. [Online]. Available: <https://www.studocu.com/row/document/abubakar-tafawa-balewa-university/petroleum-engineering/gas-lift-advanced-artificial-lift-methods/6550482>. [Accessed 30 04 2024].
- [29] N. Okon, D. Appah and a. J. U. Akpabio, "].( Water Coning Prediction Review and Control: Developing an Integrated Approach," *Journal of Scientific Research & Reports*, p. 24, 07/06/2017.
- [30] F. A. Makinde, O. A. Adefidipe and A. J. and Craig, "Water Coning in Horizontal Wells: Prediction of Post-Breakthrough Performance.," *The International Jornal of Engineering and Science*, p. 27, 2011.
- [31] K. Chan, "Water Control Diagnostic Plots," *SPE Annual Technical Conference &Exhibition*, pp. 755-763, 22-25 October, 1995.
- [32] M. C. T. Kuo and C. L. DesBrisay, "A Simplified Method for Water Coning Predictions," *SPE Annual Technical Conference and Exhibition*, October 1983.

- [33] F. Aliev, B. Amzayev and K. Rahimov, "Water coning," *researchgate*, p. 59, 2014.
- [34] Amani, A. Taha and a. Mahmood, "Overview of Water Shutoff Operations in Oil and Gas Wells; Chemical and Mechanical Solutions," *Chemical Engineering Journal*, p. 11, 14 May 2019.
- [35] M. H. Raoufi, A. Farasat and M. Mohamadifrad., "Application of simulated annealing optimization algorithm to optimal operation of intelligent well completions in an offshore oil reservoir.," *Journal of Petroleum Exploration and Production Technology*, vol. 5, pp. 1-12, octobre 2014.
- [36] C. Gao, M. Rivero, E. Nakagawa and a. G. Sanchez, "Down hole separation technology \_past, present and futur," *APPEA Journal*, p. 3, 2007.
- [37] Ibuchukwu and O. Stanley, "Techniques of Controlling Water Coning in Oil Reservoirs," *Researche gate*, p. 8, May 2015.
- [38] *Dossier Du Champ D'huile TFT Doc, Sonatrach.*
- [39] e. Petroleum, IPM PROSPER user manual, 2008.
- [40] A. M. Alkhudafi, Properties of Reservoir Rocks, cairo, 2022.
- [41] A. Ali, M. Alabdrabalnabi, M. A. Ramadan, M. S. Aljawad, A. Almohsin and a. M. Azad, "Ntional Centre for Biotechnology information," [Online]. Available: <https://www.ncbi.nlm.nih.gov/pmc/articles/PMC10993421/>. [Accessed 09 05 2024].

# *Appendices*



Appendix A: AMA 73 technical sheet

		SH / DP / T . F . T		<b>EQUIPEMENT DU PUIT</b>				FOLIO N° : 01	
CHAMP : AMA		PUITS : <b>AMA 73</b>		X : 321252,058		Y : 3177659,991			
Centre :		COMPLETION : Simple en GL		RESERVOIR : Ordovicien					
		TYPE DE PUIT : Producteur d'huile		TYPE DE PROD : Gas lift					
<b>TETE D'ERUPTION</b>									
MARQUE : FMC		TYPE : C S		Race Sup :		SUSPENSION TBG		COUPE SCHEMATIQUE	
PRESSION DE SERVICE : 5000		Attache Tbg : Olive				OLIVE : FMC		<b>DU PUIT</b> Z - FORAGE : 368.62 Z - SOL : 360.00 Z - PROD : 360.26 S P : 0.57	
EMBASSE : 11" 3000 *7" 1/16 5000		REDUCTION :				7" 1/16 * 2" 7/8 EU			
VANNES	SAS	MAITRESSE	Lat-TBG	Lat-Csg					
MARQUE	FMC	FMC	FMC	FMC	ETANCHEITE S/TBG				
NOMBRE	1	2	2	2	Neant				
DIAM ET SERIE	2" 9/16 5000	2" 9/16 5000	2" 1/16 5000	2" 1/16 5000					
<b>COLONNE DE TUBINGS</b>									
N°	DESIGNATION	NBRE	TYPE	DIAM	LONG	COTE PRD	OBSERVATIONS		
1	Sabot	1	EU	2" 7/8	1.20	1685.30	Tbg crt biseauté		
2	Siège "XN"	1	XN	2" 7/8	0.27	1684.03	OTIS Dint=55 mm		
3	Tbgs long	1	EU	2" 7/8	9.54		6.50 Lbs/ft N80 Dint=62 mm		
4	RED	1	WFD	4" 1/2	0.25		RED 4" 1/2 NAVM* 2" 7/8 EU		
5	Packer	1	WFD	7"	1.37	1673.04	WEATHERFORD HP=0,44 BP=1,37		
6	Anchor seal	1	WFD	7"	0.21				
7	Tbgs long	1	EU	2" 7/8	9.29		6.50 Lbs/ft N80 Dint=62 mm		
8	Mandrin	1	EU	2" 7/8	2.08	1663.10	Weatherford		
9	Tubings	23	WF	2" 7/8	214.21		6.50 Lbs/ft N80 Dint=62 mm		
10	Mandrin	1	EU	2" 7/8	2.08	1446.71	Weatherford		
11	Tubings	32	WF	2" 7/8	297.92		6.50 Lbs/ft N80 Dint=62 mm		
12	Mandrin	1	EU	2" 7/8	2.08	1146.71	Weatherford		
13	Tubings	30	WF	2" 7/8	279.38		6.50 Lbs/ft N80 Dint=62 mm		
14	Mandrin	1	EU	2" 7/8	2.08	865.25	Weatherford		
15	Tubings	45	WF	2" 7/8	421.93		6.50 Lbs/ft N80 Dint=62 mm		
16	Mandrin	1	EU	2" 7/8	2.08	441.24			
17	Tubings	47	EU	2" 7/8	439.49				
	Olive		EU	2" 7/8	0.35				
Total colonne					1685.81				
<b>PERFORATIONS DE PRODUCTION</b>									
Niveau perforé	Hauteur	Type de perfos	Diam	Densité	Calage	Nbre de coups tirés			
<b>OBSERVATIONS :</b> Poids de la colonne de tubings au MD = 21 Tonnes Appareil TP 200 Boue de densité D= 0,88 Csg 7" mixte de 0-1481,4 26# et de 1490 a 1854,64 29# Fiche technique établie par M : Djermouni									
Csg-13" 3/8-68# 37,64 m Csg-9" 5/8-P110#-47# Mandrin 441,24 785,64 m Mandrin- 865,25 Csg-7" P110-29# Mandrin- 1146,71 Tbg-2" 7/8 EU -6,5 # N80 Mandrin- 1446,71 Mandrin 1663,1 Packer- 1673,04 TOL 1680,64 Siege "XN"- 1684,03 Sbt Tbg- 1685,30 m Sbt 7"-1854,64m Liner 4" 1/2 P100 13,3# Anneau 2001,64 2030,64 m									
<b>ANNULE LE FOLIO N° 1</b>									
Début Reprise :		27/02/2018							
Fin Reprise :		28/02/2018							
Mise à jour le :		13/03/2018							

Appendix B: AMA 75 technical sheet

SH / DP / T . F . T		EQUIPEMENT DU Puits				FOLIO N° 1	
CHAMP : T.F.T		PUITS : <b>AMA-75</b>		X : 320 220.034m		Y : 3 176 450.003	
Centre : AMASSAK		COMPLETION : Simple		RESERVOIR : Dévonien			
		TYPE DE Puits : Producteur d'huile		TYPE DE PROD : Gas-lift			
<b>TETE D'ERUPTION</b>							
MARQUE : FMC		TYPE : C.S		Race Sup : Quick union		SUSPENSION TBG	COUPE SCHEMATIQUE
PRESSION DE SERVICE : 5000		Attache Tbg : Olive		BRIDE :		DU Puits	
EMBASE : 11" 3000		RED:		OLIVE :		Z - FORAGE : 371.660	
VANNES		SAS	MAITRESSE	Lat-TBG	Lat-Csg	Z - SOL : 363.040	
MARQUE		FMC	FMC	FMC	FMC	Z - PROD :	
NOMBRE		1	2	2	2	S P : 0.56	
DIAM ET SERIE		2"9/16 5000	2"9/16 5000	2"1/16 5000	2"1/16 5000		
<b>COLONNE DE TUBINGS</b>							
N°	DESIGNATION	NBRE	TYPE	DIAM	LONG	COTE PRD	OBSERVATIONS
1	Sabot	1	EU	2"7/8	1.20	1672.07	Tbg crt biseauté
2	Siege	1	"XN"	2"7/8	0.19	1671.88	Ouis "NO GO " Dint=56 mm
3	Manchon	1	EU	2"7/8	0.14	1671.74	6,50 Lbs/ft N80 Dint=62 mm
4	Tubing long	1	EU	2"7/8	9.37	1662.37	6,50 Lbs/ft N80 Dint=62 mm
5	Reduction	1	EU	2"7/8	0.23	1662.14	4"1/2 EU X 2"7/8 EU
6	Packer hydr	1	baker	7"	1.54	1660.60	(B=0.94 m , H=0.44 m )
7	Ratch-latch	1	baker	2"7/8	0.21	1660.39	Weatherford
8	Tubings	12	EU	2"7/8	112.30	1548.09	6,50 Lbs/ft N80 Dint=62 mm
9	Mandrin	1	W.ford	2"7/8	2.08	1546.01	Weatherford
10	Tubings	32	EU	2"7/8	299.15	1246.86	6,50 Lbs/ft N80 Dint=62 mm
11	Mandrin	1	W.ford	2"7/8	2.08	1244.78	Weatherford
12	Tubings	37	EU	2"7/8	345.12	899.66	6,50 Lbs/ft N80 Dint=62 mm
13	Mandrin	1	W.ford	2"7/8	2.08	897.58	Weatherford
14	Tubings	43	EU	2"7/8	401.08	496.50	6,50 Lbs/ft N80 Dint=62 mm
15	Mandrin	1	W.ford	2"7/8	2.08	494.42	Weatherford
16	Tubings	53	EU	2"7/8	494.09	0.33	6,50 Lbs/ft N80 Dint=62 mm
17	Olive	1	EU	2"7/8	0.33	0.00	FMC- 7"1/16 OD * 2"7/8 EU
<b>Total garniture</b>						<b>1673.27</b>	
<b>PERFORATIONS</b>							
Niveau Perforé	Hauteur	Diamètre Perfos	Densité/m	Type de Perfos			
<b>OBSERVATIONS :</b>							
Poids de la garniture au MD =19 tonnes dans une boue (OBM) d = 0,94 V = 46							
Appareil TP 200							
ETABLIE PAR: M BOUREGA D.BEHADRI							

<b>ANNULE LE FOLIO N°</b>	
Début Completion : 03/06/2018	
Fin Completion : 05/06/2018	
Mise à jour le : 06/06/2018	

Appendix C: PVT matching data

Input Data

Input	Options	Composition	Warnings
Solution GOR	164.797		Sm3/Sm3
Oil Gravity	41.061		API
Gas Gravity	0.87394		sp. gravity
Water Salinity	182000		ppm
Mole Percent H2S	0		percent
Mole Percent CO2	0.7		percent
Mole Percent N2	2.38		percent
Pb, Rs, Bo Correlation	Standing		
Oil Viscosity Correlation	Beggs et al		

PVT Match data

Table 1

Temperature: 80 deg C  
Bubble Point: 177.577 BARg

Point	Pressure	Gas Oil Ratio	Oil FVF	Oil Viscosity
	(BARg)	(Sm3/Sm3)	(m3/Sm3)	(mPa.s)
1	0	0	1.03314	1.36876
2	39.2249	28.8379	1.12984	0.52458
3	58.8374	45.2735	1.17576	0.44308
4	98.0621	79.9778	1.27088	0.32823
5	137.287	118.695	1.37544	0.24705
6	156.9	140.178	1.4332	0.21427
7	177.577	164.797	1.49921	0.18386
8	186.318	164.797	1.49458	0.18725
9	220.64	164.797	1.47782	0.20044
10	269.671	164.797	1.45711	0.21892
11				
12				
13				
14				
15				

Appendix D: IPR matching data

Rate Type						Adjust IPR	
Oil Rate						Adjust IPR	
Match Data							
Test	Test Point Date	Test Point Comment	Tubing Head Pressure	Tubing Head Temperature	Water Cut	Oil Rate	
			(BARg)	(deg C)	(percent)	(Sm3/day)	
1	07/08/2018		6.7	37	0	4.7	
2	17/08/2018		5.4	37	0	9.5	
3	18/10/2018		16	37	5.6	25.5	
4	19/10/2018		16	37	26.1	18.4	
5	13/02/2019		6.2	37	0	35.8	
6	29/10/2019		8.1	37	16.2	16	
7	07/02/2020		9.7	37	26.2	7.9	
8	14/02/2020		11	37	33.3	6.4	
9	18/08/2020		9.1	37	22.1	12	
10	13/02/2021		10.9	37	34.4	12	
11	02/08/2021		9.2	37	34	6.2	
12	29/12/2021		7.6	37	33.3	4.8	
13	09/09/2023		114.6	37	16.9	27.6	

Gas Oil Ratio	GOR Free	Gaslift Gas Rate	Injection Depth (Measured)	Casing Head Pressure
(Sm3/Sm3)	(Sm3/Sm3)	(1000Sm3/d)	(m)	(BARg)
21	0	3.917	1446.71	46
53	0	6.908	1446.71	53
0	0	9.2	1446.71	42
260	0	9.2	1446.71	42
3	0	9.915	1446.71	28
418	0	16.74	1446.71	29
1256	0	10.36	1446.71	32
1449	0	10.369	1446.71	30
8	0	16.726	1446.71	42
403	0	16.753	1446.71	38
726	0	15.555	1446.71	33
2174	0	11.03	1446.71	26
7485	0	0	1446.71	0

Appendix E: Gas lift input data

Options		Gaslift Details	
Gas Lift Type	No Friction Loss In Annulus Friction Loss In Annulus Model Safety Equipment	Gaslift Valve Depth (Measured)	1446.71 m
Gas Lift Method	Fixed Depth of Injection Optimum Depth of Injection Valve Depths Specified	Injection Point	Injection Point is ORIFICE
Input Method	Use GLR Injected Use Injected Gas Rate	Orifice Diameter	6.35 mm
		Thornhill-Craver DeRating	90 percent
Input Data			
Gaslift Gas Gravity	0.732	sp. gravity	
Mole Percent H2S	0	percent	
Mole Percent CO2	0	percent	
Mole Percent N2	0	percent	
Injected Gas Rate	16.753	1000Sm3/d	